Fire-Induced Radiological Integrated Assessment

Fire properties of selected materials and products

Madsen, Dan; Barton, John; van Hees, Patrick; Malmborg, Vilhelm; Gren, Louise; Gudmundsson, Anders; Pagels, Joakim

2019

Document Version:
Publisher's PDF, also known as Version of record

Fire-Induced Radiological Integrated Assessment – Fire properties of selected materials and products

WP-AT: T-LU-AD_FD-01 Soot Testing Campaign: Deliverables FD03

Date: 13th of September 2019

Dan Madsen, John Barton & Patrick van Hees
Division of Fire Safety Engineering, Faculty of Engineering, Lund University

&

Vilhelm Malmborg, Louise Gren, Anders Gudmundsson and Joakim Pagels
Division of Ergonomics & Aerosol Technology,
Faculty of Engineering, Lund University

LUND UNIVERSITY

Summary

Characterization of emissions from fires in a laboratory-controlled environment are presented in this report. The project is initiated by the CERN HSE Unit and is called FIRIA, Fire-Induced Radiological Integrated Assessment. The objective of FIRIA is to enhance the knowledge of aerosols emitted from fires in order to develop dispersion models of radiologically-activated material in case of fire. In this report, several normally occurring combustible products and materials are tested in a standardized setup for fire tests, the cone calorimeter. In the cone calorimeter, standardized fire tests according to ISO 5660-1:2015 have been performed as well as fire tests at reduced oxygen concentrations in a vitiated air chamber. As an additional setup, aerosol measurement equipment was coupled to the cone calorimeter ventilation duct to characterize the emitted aerosols as in the particle size distribution, mass yield and elemental analysis.

The results show peak heat release rates for oil at 1100 kW/m^2 at an incident heat flux of 50 kW/m^2. Similar results for the plastic materials were 800 kW/m^2. For cables and insulating plastic materials peak heat release rates at an incident heat flux of 50 kW/m^2 were around 350 kW/m^2. Significant for most of the cables was a heat release rate curve with two distinct peaks. This is proposed to be due to the outer combustible sheath burning first followed by the interior plastic insulating material of the cables burning. There could also be heat transfer effects and cracking of the material surface contributing to the two peaks. Nevertheless, for some cables a low incident heat flux led to only one peak indicating that only the sheath ignited. Time to ignition varied between the materials but was increased as the incident heat flux decreased. Reduced oxygen concentration in the vitiated air chamber also prolonged the ignition time as well as the heat release rates. The critical heat flux to ignite the cables was calculated to be just below 10 kW/m^2. The oil and two cable types were tested in the vitiated air chamber to perform tests at reduced oxygen concentrations. These tests were performed to retrieve specific fire properties as well as specific emissions from such conditions. The tests were performed with a progressively lower oxygen concentrations until no ignition of the sample occurred. Results showed an ignition limit around 11-13 % oxygen at incident heat fluxes of 20-30 kW/m^2. The tests in the vitiated air chamber is described in subreport FIRIA- Fire properties of selected materials and products in reduced oxygen conditions.

Contents

1 Introduction

Dangers connected to fire and emissions from fires have basically been related to fire spread, heat exposure and toxic gases as well as reduced visibility conditions. The CERN HSE Unit has extended the research within the area of emissions from fires in the project FIRIA, Fire-Induced Radiological Integrated Assessment. The objective is to enhance the knowledge of aerosols emitted from fires at specific conditions. In this report, standardized fire tests at laboratory-controlled conditions were performed to determine the emitted aerosols specifics as particle size distribution, mass yield as well as elemental analysis of collected filter samples. This information will then be used to develop dispersion models to predict emission releases from fires.

1.1 Materials and products

Tested materials and products have been chosen due to being commonly used and present at CERN facilities. The materials in the products are mainly plastics except for an oil. The products can be divided into cables, plastic sheets of different thicknesses, electrical cards, isolated magnets and an oil. The cables are both multi-conductors and with a single metal core. The materials and products are presented in 5 Appendix.

1.2 Experimental setup

To conduct the tests in laboratory-controlled fire conditions, the cone calorimeter [1] was used in its base design and in the oxygen-reduced tests, with a coupled vitiated air chamber [2]. An ISO-standard for these tests in vitiated conditions is not approved yet, therefore the procedure by Werrel et al. [3] was used. The aerosol measurement was done with equipment connected to the standard soot sampling connection in the cone calorimeter ventilation duct. The dilution was set-up in two stages after a pre-cyclone (nominal cut-off diameter ~5-7µm). The primary dilution (dilution factor ~30) was conducted using a porous tube diluter and ejector diluter in series. Secondary dilution was conducted using rotating disc diluters connected prior to the Aethalometer that required lower PM concentration. At the tests with the oxygen-reduced conditions, a vitiated air chamber with a standardized metallic chimney [4] (ISO 13927) was used to prevent backflow of gases and avoid flames burning in ambient air. The chimney has four thermocouples for estimating the heat release that could be used according to the standard. Nevertheless, the oxygen depletion technique in ISO 5660-1:2015 [5] for determining heat release was used. The experimental setup is schematically presented in Figure 1.

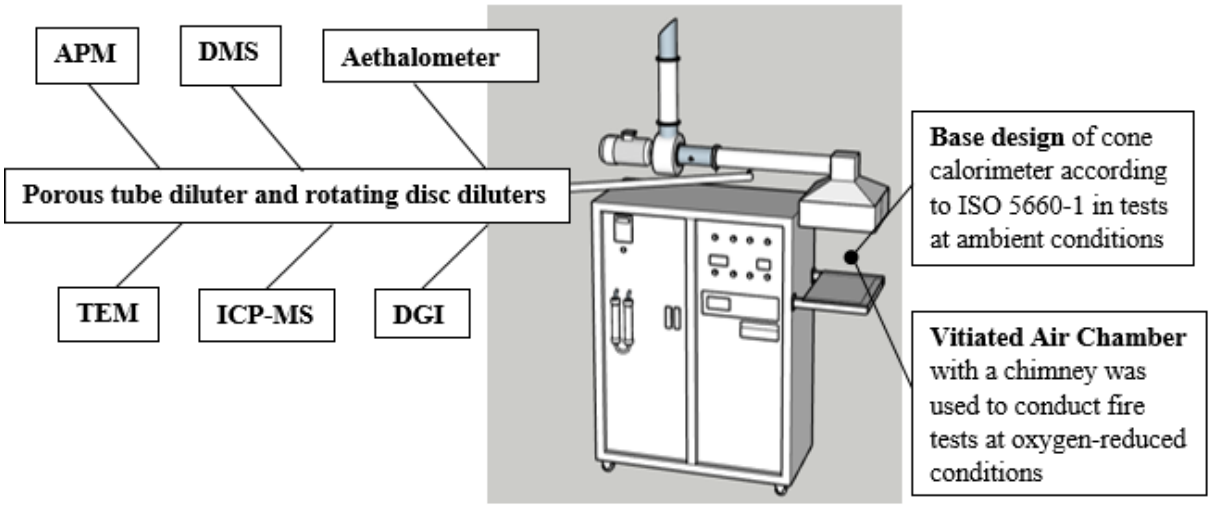

Figure 1. Schematic setup of the equipment.

A **Vitiated air chamber, VAC,** was used for oxygen reduced conditions. The chamber was fed with a continuous gas flow of controlled conditions. The flow of pressurized air and nitrogen was controlled by mass flow controllers. Two oxygen analysers were placed to show the oxygen content after mixing the gases as well as to measure the oxygen content in the vitiated air chamber.

Porous tube diluter and rotating disc diluters were used to arrange measurable conditions in the analysis equipment.

The **APM**, Aerosol Particle Mass analyser, was used to determine particle effective densities. A **DMA**, Differental Mobility Analyser was used prior to the APM to size-select the particles in order to measure the effective density of the selected particle sizes.

The **DMS,** Differential Mobility Spectrometer, determined the particle number size distribution.

Through the use of the **Aethalometer**, the black carbon (soot) concentration was determined by light attenuation at 7 wavelengths in the IR-VIS-UV spectrum.

With the **TEM,** Transmission Electron Microscopy, the particles were imaged so the soot structure could be analysed.

The **ICP-MS**, Inductively Coupled Plasma Mass Spectrometry**,** was used for elemental determinations.

The **DGI**, Dekati Gravimetric Impactor, sampled the aerosols in four stages to present an aerodynamic particle mass size distribution.

1.3 Method

All tested items were placed in a sample holder according to the standard procedure (ISO 5660-1:2015) in cone calorimeter tests. CO- and CO_2-yields are calculated according to Janssens and Parker [6]. Cables were cut in lengths of 105 mm, products larger than the sample holder were cut with dimensions of 105x105 mm as presented in Figure 2. Cable ends were not sealed. Oils were poured in the lower part of the sample holder with an adjusted height to not hinder the movement of the igniter. The upper part of the sample holder was not used for the test of fluids. All tests were recorded with video camera for better understanding of the fire behaviour.

Figure 2. Example of cables in sample holder prior to test.

Usage of the experimental setup was coordinated by communication between operators of the cone calorimeter and of the aerosol measurement equipment. For data sampling, the cone calorimeter software, ConeCalc, was used as well as recordings for aerosol results. Test procedures varied as specific equipment was used but two general procedures are presented:

(1) Test procedure for well-ventilated conditions. This test procedure was used for most of the tests and the experimental setup was a normal setup according to ISO 5660-1:2015 with an aerosol sampling/dilution tube connected to the soot sampling connection at the cone calorimeter ventilation duct.
(2) Test procedure for vitiated air conditions. This test procedure was used to generate conditions of reduced oxygen due to a higher content of inert gas, as nitrogen in these tests.

1.3.1 Test procedure for well-ventilated conditions

1. The real time at start of baseline was documented as the baseline was started in ConeCalc and the recording of aerosol-measurements were started. Baseline sampling of ambient conditions was for at least 60 seconds.
2. After baseline was collected, the sample holder was inserted on the load cell - igniter was positioned above sample surface. Simultaneously, the protection shield and Start test-button was pushed to expose the sample surface to the heat flux. The exterior protection shield of the cone calorimeter was then lowered.
3. Time to ignition was documented in ConeCalc and in aerosol-measurement protocol. DGI was started at ignition at specific tests.
4. 120 seconds after ignition, APM was started and starting time documented.
5. At flameout, DGI was stopped but APM continued to sample for 30 minutes after ended test.
6. Data sampling was collected approximately 120 seconds after flameout before the test was ended in ConeCalc.

1.3.2 Test procedure, vitiated air chamber, see subreport FIRIA- Fire properties of selected materials and products in reduced oxygen conditions.

1.3.3 Critical heat flux

Determining a minimum critical heat flux for ignition of thermally thick wood products has earlier been performed by Janssens [7]. Janssens also made a reappraisal [8] of determining the critical heat flux to be extended to a wider range of materials as plastic material, PMMA. In this reappraisal, Janssens plots the inverse of time to ignition at the power of 0,55 against the irradiance of the specific cone calorimeter test on the horizontal axis. By using at least three tests, the extension of the linear fit presents the critical heat flux where the line crosses the horizontal axis. An example of using the method for cable 1 is shown in Figure 3. Results from this method are based on assumptions as that the thermal properties are constant and that the material is thermally thick. Using this method with cables consisting of both plastics and metals as well as with varying diameters means that the results should be handled with caution. Nevertheless, the method is used and evaluated for the cables in this testing campaign that have been tested and ignited at minimum of three different heat fluxes in ambient air.

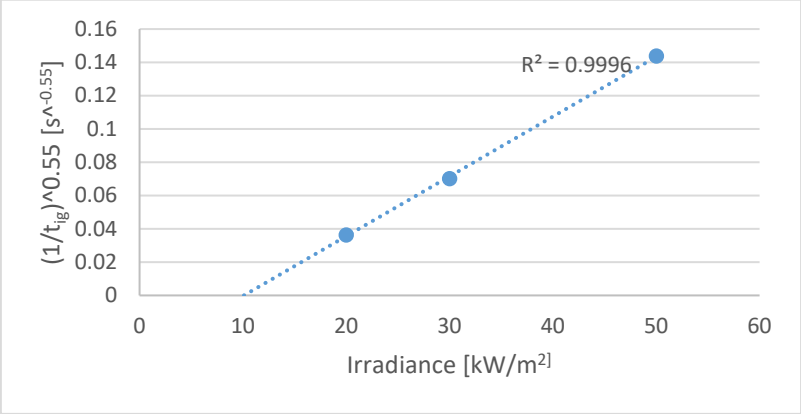

Figure 3. Determining the critical heat flux of cable 1.

2 Results

The reduced results are introduced in this chapter. All the tests with comments are briefly presented in an Excel-sheet but an extract is presented here for each item to give an overview of measurements taken. All reports, data sampling, reduced data, photos, videos and pictures are stored electronically at https://lu.app.box.com/folder/69299876673. A table over the tested items are presented in 5 Appendix.

The resulting fire properties, obtained from the cone calorimeter measurements, are presented in this chapter for each test.

As a screening test, Cable 4, C04, was tested both with sealed ends and unsealed but without any change in fire behaviour that not can be explained by usual variation in fire tests. The used sealant was a firestop sealant for building products. Nevertheless, as there were no considerable changes between the tests, all following cable tests were performed with unsealed ends.

In 2.17, the critical heat fluxes are presented for some of the cables.

Attempts to measure the ignition temperature at the surface of the sample with a thermocouple were made but the measurement resulted in disturbances to the mass loss measurement so the ignition temperature measurement was not done for all tests.

2.1 Cable 1, C01

Cable 1 is a blue multi conductor cable with a thermoset insulator and an outer diameter of 9.3 mm. The sales marking is DRAKA 14W20 CERN MCA 14 IEC 60332-1 ZERO HALOGEN 09 3212577 405130804 3160 MT. The cable was tested in three tests according to Table 1.

Table 1. Performed tests of Cable 1, C01.

Test	Heat flux (kW/m^2)	DMS	Aethalo-meter	DGI	APM	TEM	ICP-MS	VAC	File name
T15	50	yes	yes	no	yes	no	no	no	T15_C01_50_1L_US
T19	30	yes	yes	yes	yes	no	no	no	T19_C01_30_1L_US
T24	20	yes	yes	no	yes	no	no	no	T24_C01_20_1L_US

Cable 1 is presented in Figure 4, showing the typical consisting parts of the tested cables.

Figure 4. The cables consist of a sheath, metallic shielding and the conductor(s) with insulating material.

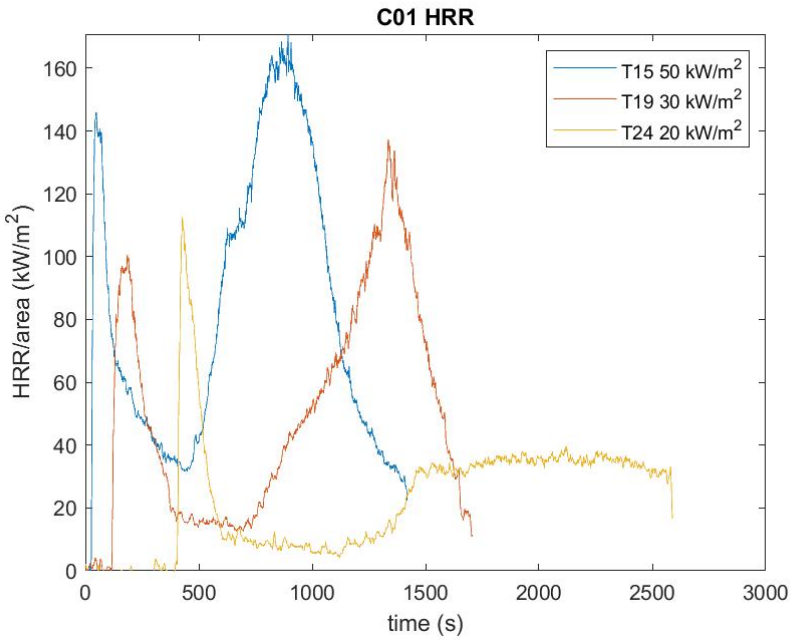

Figure 5. Heat release rates per unit area of Cable 1 at different heat fluxes.

Cable 1 was tested at three heat flux levels as presented in Figure 5. The graphs show a bimodal behaviour as first the sheath of the cable is ignited and then the insulation material of the conductors is ignited. At some occasions at low heat fluxes, the sample was extinguished after the first ignition of the sheath as the conduction of heat was not enough to an immediate ignition of the conductors. This is the case in T19 and T24. There the samples are extinguished after the first ignition of the sheath, the igniter was inserted and after a phase with heat conducting to the interior of the cable, the insulation material of the conductors is ignited. Following graphs, Figure 6 and Figure 7, show the mass loss rates and obscuration in the tests.

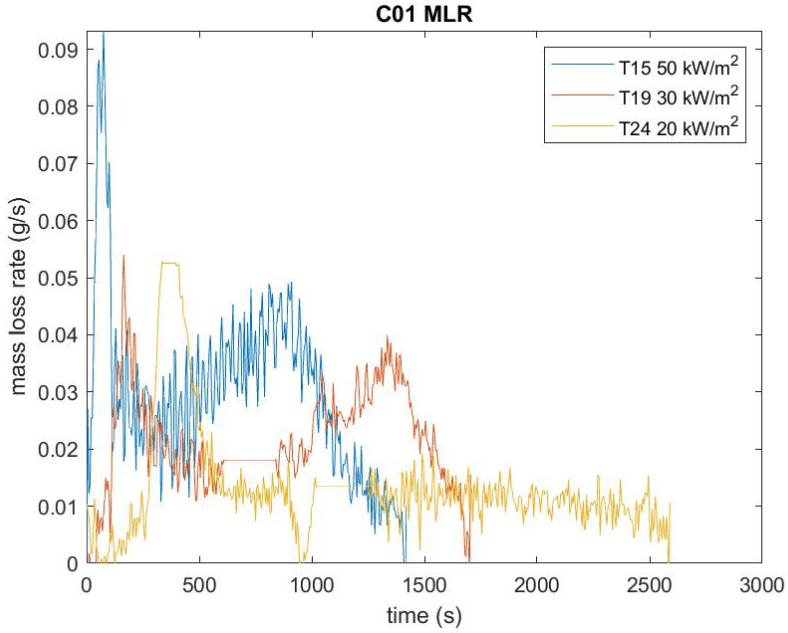

Figure 6. Mass loss rate of Cable 1 at different heat fluxes.

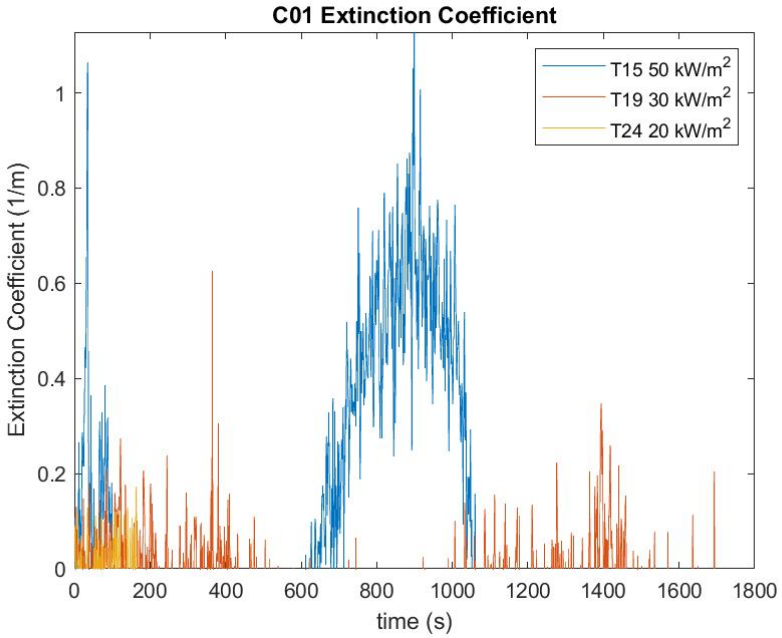

Figure 7. Obscuration for Cable 1 at different heat fluxes.

Figure 8 shows the time dependent values of heat of combustion during each test.

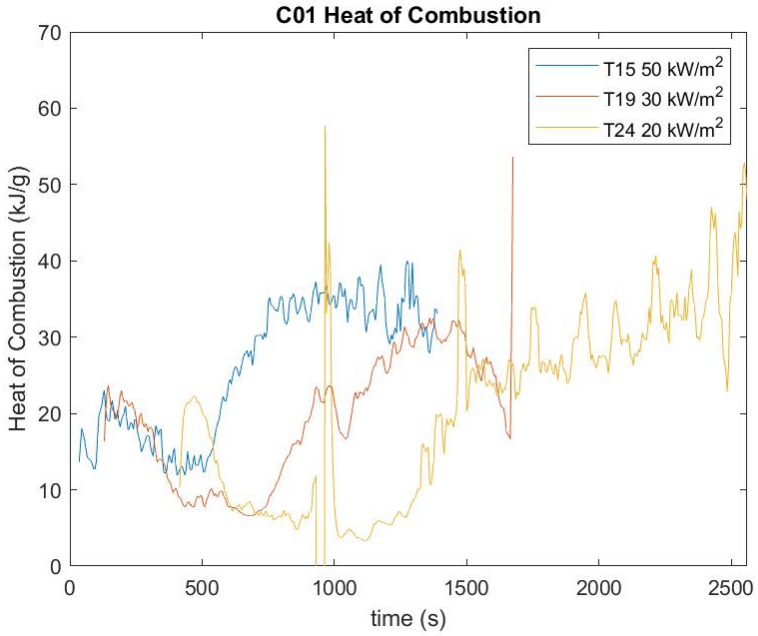

Figure 8. Heat of Combustion from ignition to 30 seconds before end of test.

In Table 2, the resulting fire properties are presented for each test. The yields and heat of combustion are calculated as average values for the whole duration of the test. For T19 and T24, it should be noted that the samples were extinguished between the combustion of the sheath and insulation material of the conductors. This intermittent burning process affects the yields and heat of combustion as the burning process were interrupted.

Table 2. Fire properties for Cable 1 at different heat fluxes.

Test	Heat flux [kW/m2]	Time to ignition [s]	CO2-yield [kg/kg]	CO-yield [kg/kg]	Heat of Combustion [MJ/kg]
T15	50	34	1.67	0.033	24.46
T19	30	125	1.37	0.073	20.54
T24	20	413	1.29	0.089	18.99

2.2 Cable 2, C02

Cable 2 is a black multi conductor cable with a thermoset insulator and an outer diameter of 14 mm. The sales marking is ELETTRONICA CONDUTTORI - 13W19 - CERN PG5SJ - IEC 60332-3-24 ZERO HALOGEN MT 0782. The cable was tested in three tests according to Table 3.

Table 3. Performed tests of Cable 2, C02.

Test	Heat flux [kW/m²]	DMS	Aethalo-meter	DGI	APM	TEM	ICP-MS	VAC	File name
T16	50	yes	yes	no	yes	no	no	no	T16_C02_50_1L_US
T20	30	yes	yes	yes	yes	no	no	no	T20_C02_30_1L_US
T25	20	yes	yes	no	no	no	no	no	T25_C02_20_1L_US

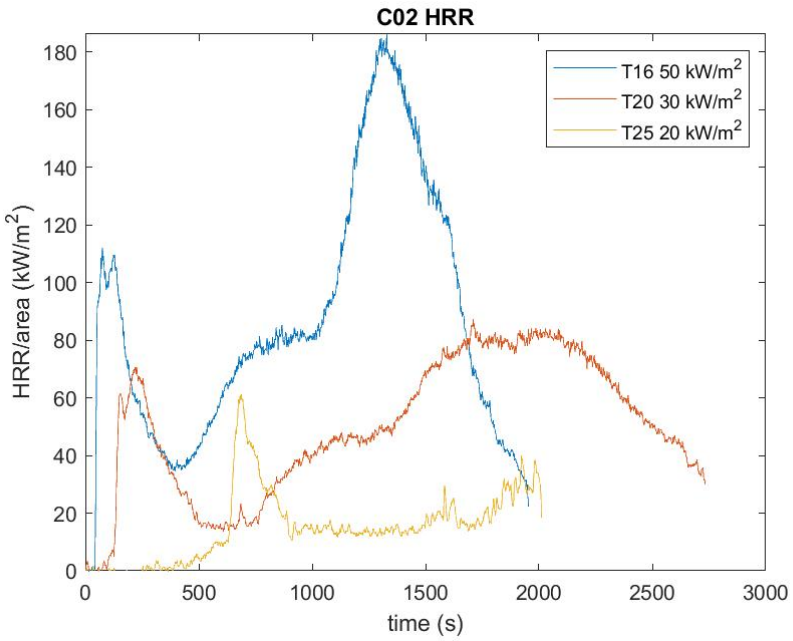

Figure 9. Heat release rates per unit area of Cable 2 at different heat fluxes.

Cable 2 was tested at three heat flux levels as presented in Figure 9. The graphs show a bimodal behaviour as first the sheath of the cable is ignited and then the insulation material of the conductors is ignited. In T25, there is a first peak when the sheath is burning and then the sample is nearly extinguished but continues to burn with a small flame until the test was stopped. Apparently, the low incident heat flux of 20 kW/m^2 was not enough to contribute to a second peak as in T16 and T20.

The following graphs, Figure 10 and Figure 11, show the mass loss rates and obscuration of the tests.

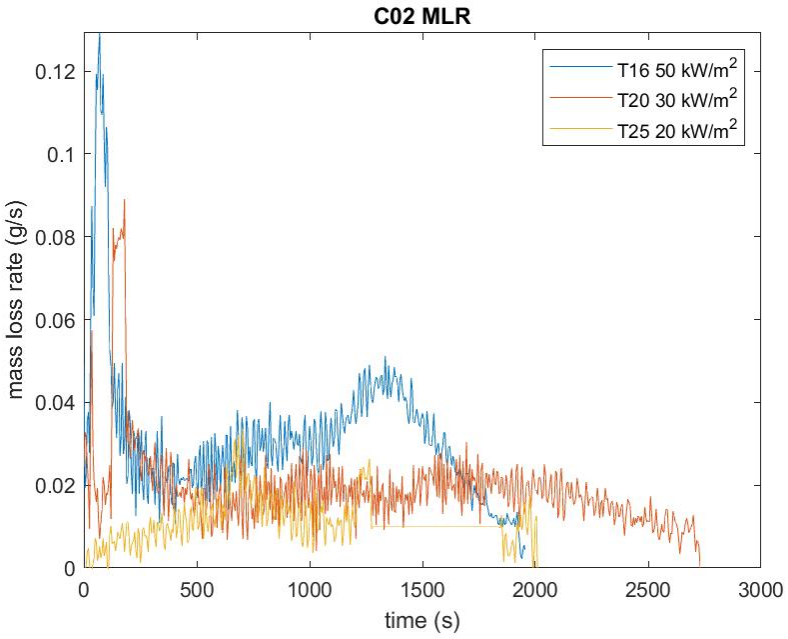

Figure 10. Mass loss rate of Cable 2 at different heat fluxes.

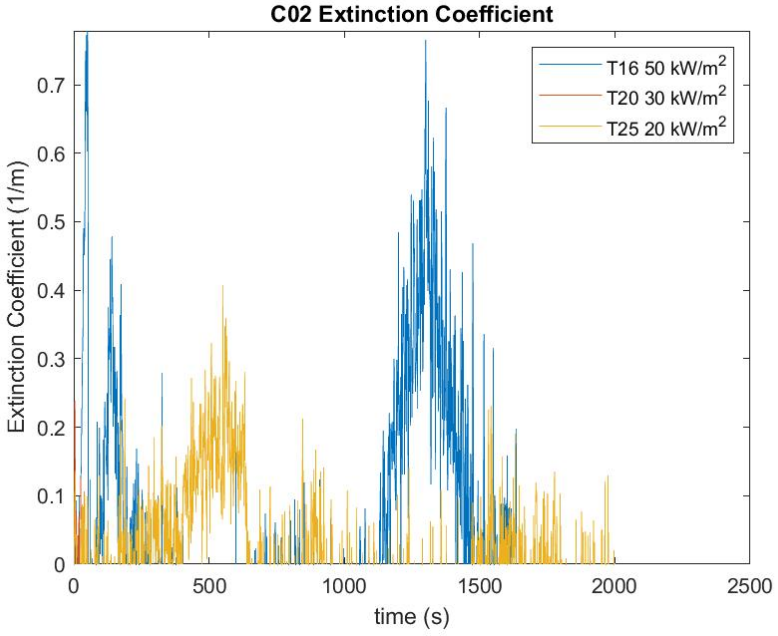

Figure 11. Obscuration for Cable 2 at different heat fluxes.

Figure 12 shows the time dependent values of heat of combustion during each test.

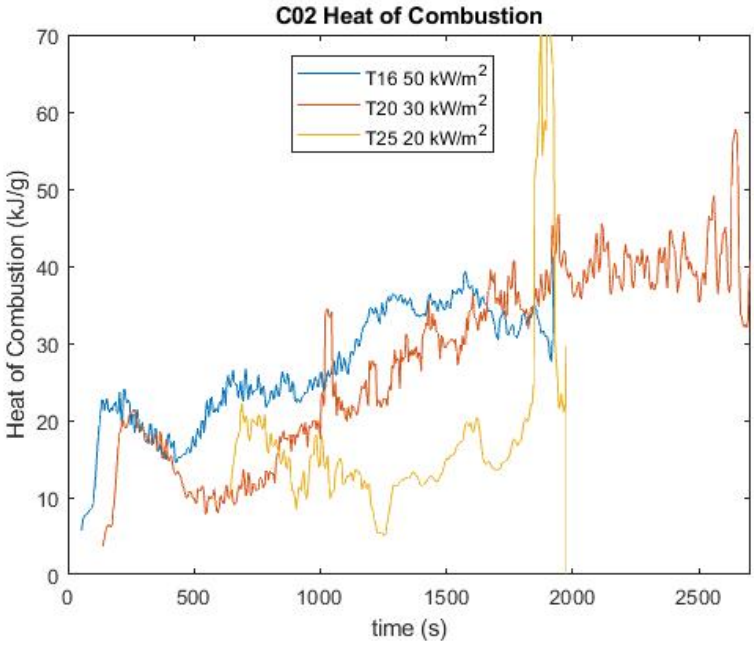

Figure 12. Heat of Combustion from ignition to 30 seconds before end of test.

In Table 4, the resulting fire properties are presented for each test. The yields and heat of combustion are calculated as average values for the test. For T20 and T25, it should be noted that the samples were extinguished between the combustion of the sheath and insulation material of the conductors. This intermittent burning process affects the yields and heat of combustion as the burning process were interrupted.

Table 4. Fire properties of Cable 2 at different heat fluxes.

Test	Heat flux [kW/m2]	Time to ignition [s]	CO2-yield [kg/kg]	CO-yield [kg/kg]	Heat of Combustion [MJ/kg]
T16	50	51	1.71	0.026	25.11
T20	30	137	1.63	0.052	25.19
T25	20	642	0.89	0.135	14.93

2.3 Cable 3, C03

Cable 3 is a red coax cable with thermoplastic dialectric insulator and an outer diameter of 10.3 mm. The sales marking is CAB.SIG.BL. 1x4x1,0 mm^2 NG4. The cable was tested in three tests according to Table 5.

Table 5. Performed tests of Cable 3, C03.

Test	Heat flux [kW/m^2]	DMS	Aethalo-meter	DGI	APM	TEM	ICP-MS	VAC	File name
T17	50	yes	yes	no	yes	no	no	no	T16_C02_50_1L_US
T21	30	yes	yes	yes	yes	no	no	no	T20_C02_30_1L_US
T26	20	yes	yes	no	no	no	no	no	T25_C02_20_1L_US

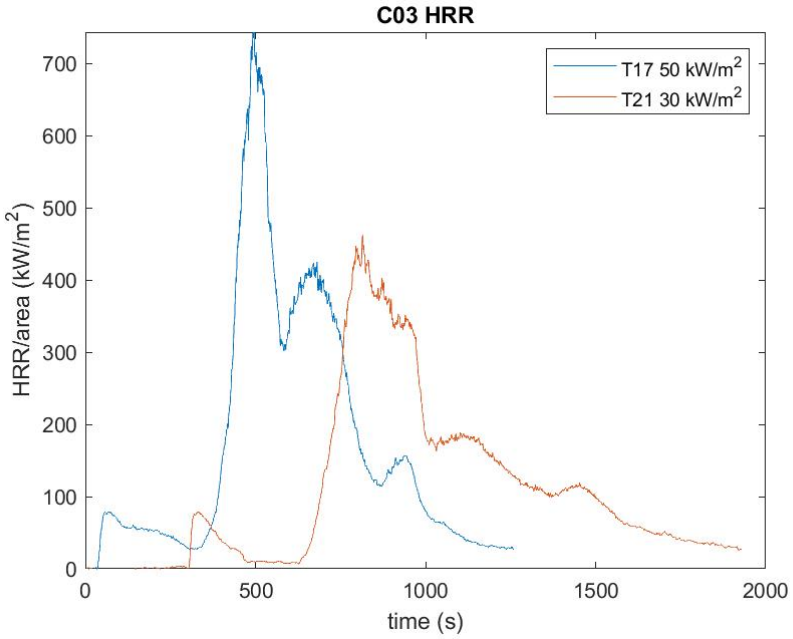

Figure 13. Heat release rates per unit area of Cable 3 at different heat fluxes.

Cable 3 was tested at three heat flux levels, however the test at an incident heat flux of 20 kW/m^2 the cable did not ignite. The other two tests are presented in Figure 13. The graphs show a bimodal behaviour as first the sheath is ignited and then the insulation material of the conductors is ignited. In T17 there were some dripping from the sample holder, about 3 grams of plastic material. This dripping behaviour could cause a potential pool fire in a full scale scenario. T21 resulted in first an ignition of the sheath followed by flameout. The igniter was then inserted again and after a while, the sample was ignited and resulted in a second peak. T26 did not ignite at all, probably due to low incident heat flux. A disturbance in igniting T26 could also be that a thermocouple was attached with tape and hindered some of the pyrolysis gases to reach the igniter. The igniter was relocated to a more favourable place for igniting the sample at the end of the test but still the sample was not ignited.

The following graphs, Figure 14 and Figure 15, show the mass loss rates and obscuration at the tests.

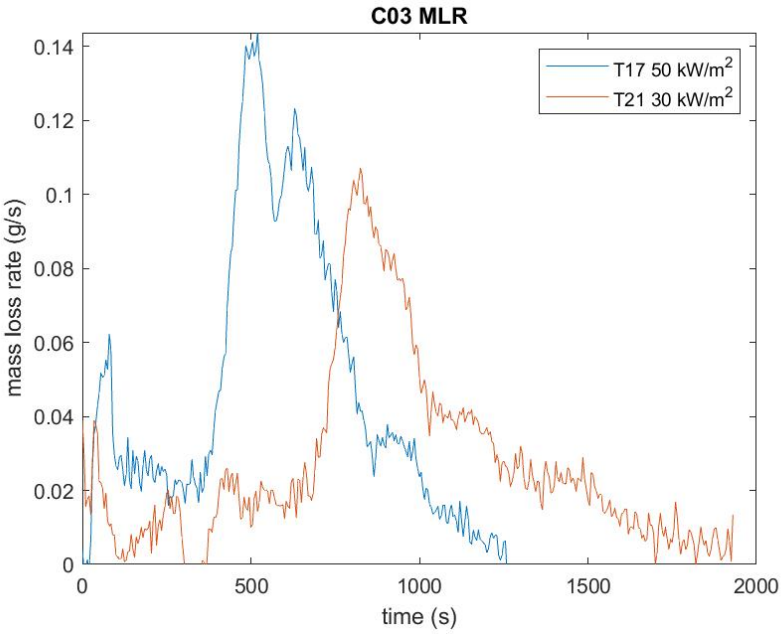

Figure 14. Mass loss rate of Cable 3 at different heat fluxes.

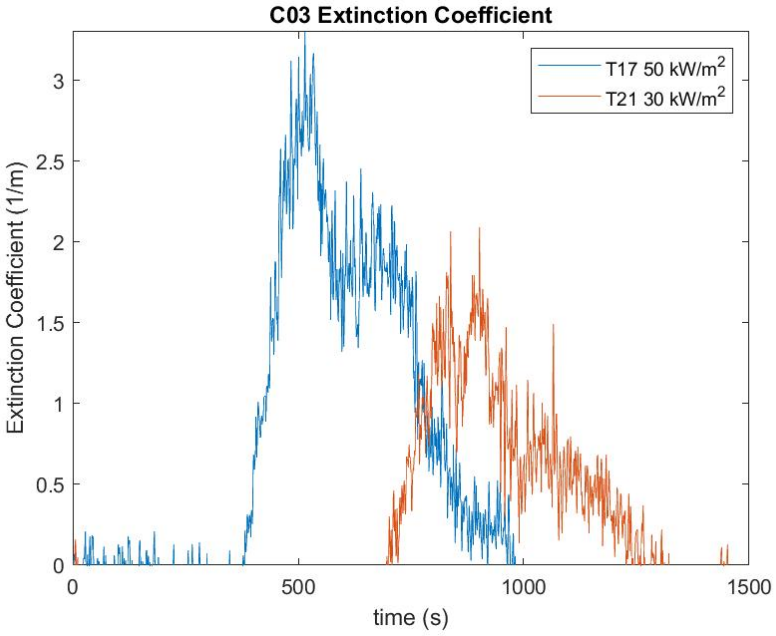

Figure 15. Obscuration of Cable 3 at different heat fluxes.

Figure 16 shows the time dependent values of heat of combustion during each test.

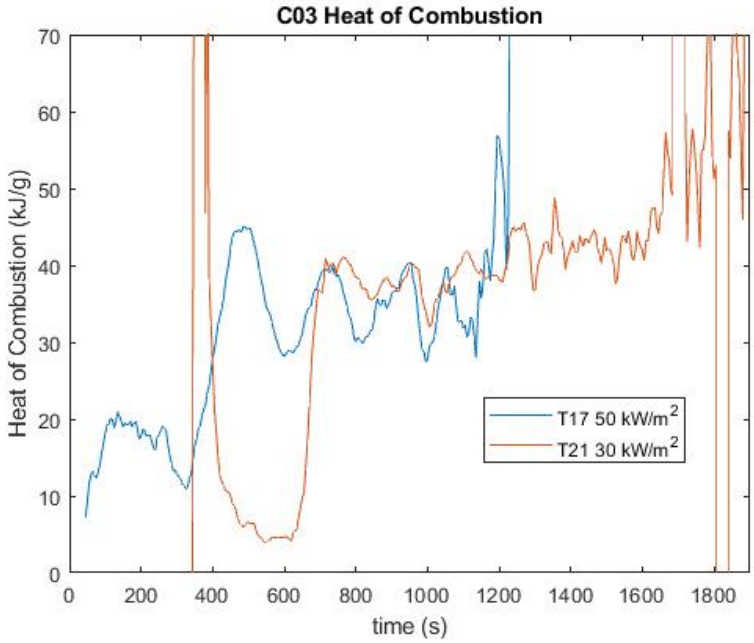

Figure 16. Heat of Combustion from ignition to 30 seconds before end of test.

In Table 6, the resulting fire properties are presented for each test. The yields and heat of combustion are calculated as average values for the test. For T21, it should be noted that the sample were extinguished between the combustion of the sheath and insulation material of the conductors. This intermittent burning process affects the yields and heat of combustion as the burning process were interrupted.

Table 6. Fire properties of Cable 3 at different heat fluxes.

Test	Heat flux [kW/m2]	Time to ignition [s]	CO2-yield [kg/kg]	CO-yield [kg/kg]	Heat of Combustion [MJ/kg]
T17	50	44	2.11	0.029	32.97
T21	30	311	2.34	0.049	37.58
T26	20	No ignition	-	-	-

2.4 Cable 4, C04

Cable 4 is a brown coax cable with a thermoplastic dialectric insulator and an outer diameter of 5 mm. The sales marking is DRAKA 2016 CB 50 09 3414713 6111308426187 MT. The cable was tested in six tests according to Table 7.

Table 7. Performed tests of Cable 4, C04.

Test	Heat flux [kW/m^2]	DMS	Aethalo-meter	DGI	APM	TEM	ICP-MS	VAC	File name
T1	50	yes	yes	no	no	no	no	no	T1_C04_50_1L_us
T2	50	yes	yes	yes	yes	no	no	no	T2_C04_50_1L_s
T4	30	yes	yes	no	yes	no	no	no	T4_C04_30_1L_us
T5	20	yes	yes	no	no	no	no	no	T5_C04_20_1L_us
T22	30	yes	yes	yes	yes	no	no	no	T22_C04_30_1L_US
T52	30	yes	yes	no	yes	no	no	no	T52_C04_30_1L_US

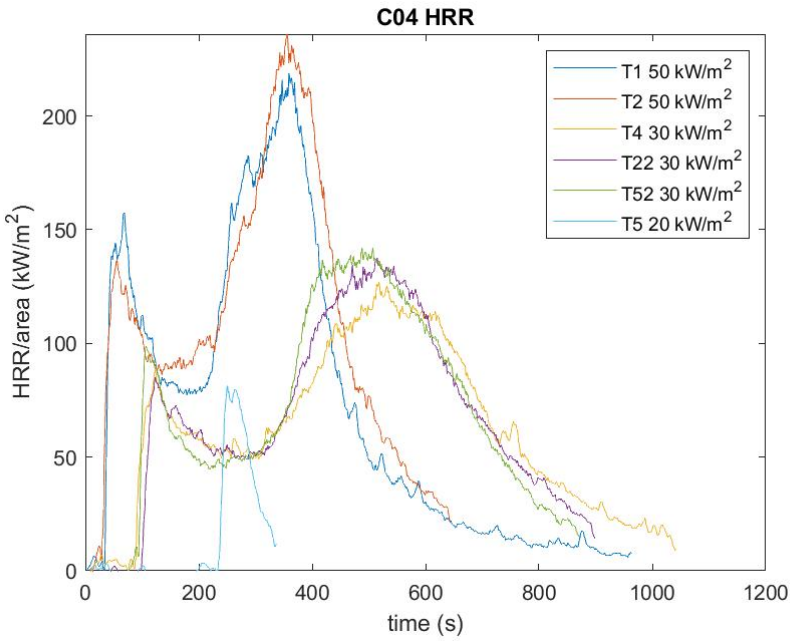

Figure 17. Heat release rates per unit area of Cable 4 at different heat fluxes.

Cable 4 was tested six times at three different heat flux levels as presented in Figure 17. The graphs shows a bimodal behaviour as first the sheath is ignited and then the insulation material is ignited. T2 was the only test performed with sealed cable ends (fire sealing for building products) in order to evaluate if the cut end-section affects the fire behaviour. Comparing the HRR between T2 (sealed cable ends) and T1 (unsealed cable ends) that was performed at same heat flux shows no specific change in the fire behaviour. This led to all other cable tests being performed with unsealed cable ends. In T5, the incident heat flux was not enough to cause an ignition of the insulation material of the conductors and result in a second peak as in the other tests.

The following graphs, Figure 18 and Figure 19, show the mass loss rates and obscuration for the tests.

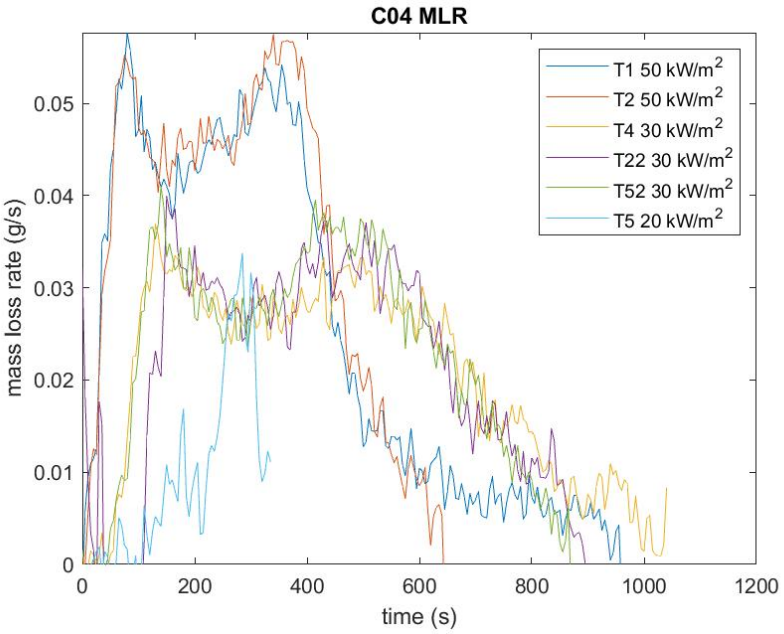

Figure 18. Mass loss rate of Cable 4 at different heat fluxes.

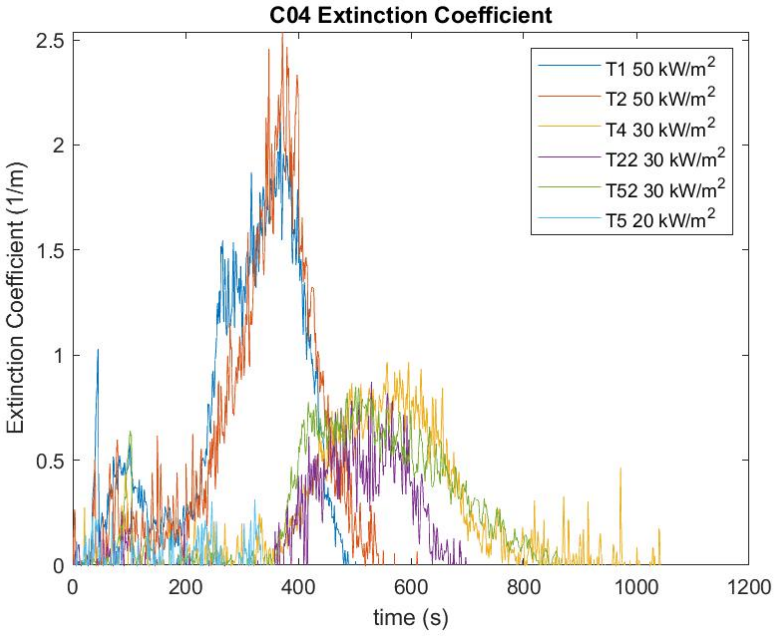

Figure 19. Obscuration of Cable 4 at different heat fluxes.

Figure 20 shows the time dependent values of the heat of combustion during each test.

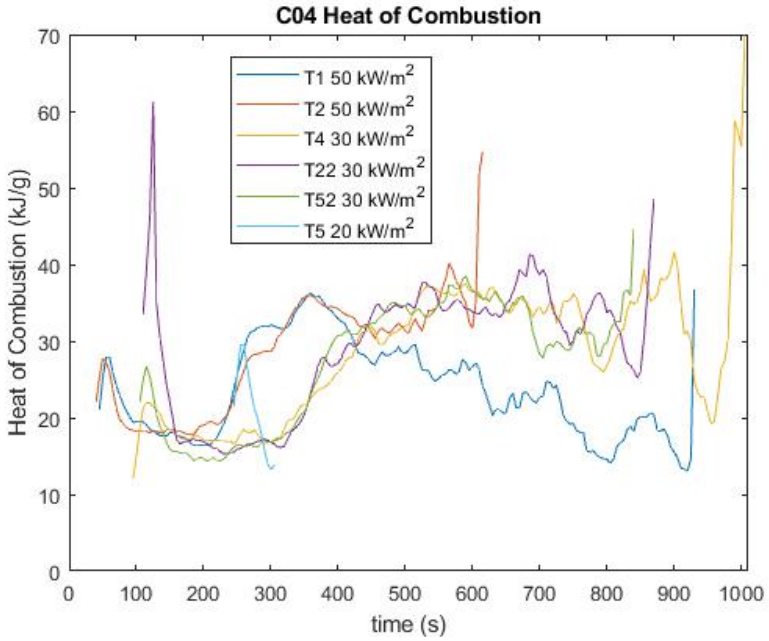

Figure 20. Heat of Combustion from ignition to 30 seconds before end of test.

In Table 8, the resulting fire properties are presented for each test. The yields and heat of combustion are calculated as average values for the test. For T5, it should be noted that the sample were extinguished after the combustion of the sheath, the test continued with pyrolysis of the cables but the insulation material of the conductors were never ignited. This intermittent burning process affects the yields and heat of combustion as the burning process were interrupted.

Table 8. Fire properties of Cable 4 at different heat fluxes.

Test	Heat flux [kW/m2]	Time to ignition [s]	CO2-yield [kg/kg]	CO-yield [kg/kg]	Heat of Combustion [MJ/kg]
T1	50	43	1.76	0.049	25.48
T2	50	39	1.87	0.036	26.80
T4	30	93	1.95	0.054	27.20
T5	20	243	1.10	0.033	17.52
T22	30	105	1.99	0.035	28.71
T52	30	103	1.76	0.050	26.06

2.5 Cable 5, C05

Cable 5 is a multi conductor cable with thermoset insulator and an outer diameter of 7 mm. The sales marking is DRAKA 16W04 CERN NE2 IEC 60332-1 ZERO HALOGEN 09 3213839 601291328 3876 MT. The cable was tested in the cone calorimeter in four tests according to Table 9. Test 23 were performed twice due to a malfunction of the DMS equipment.

Table 9. Performed tests of Cable 5, C05.

Test	Heat flux [kW/m²]	DMS	Aethalo-meter	DGI	APM	TEM	ICP-MS	VAC	File name
T18	50	yes	yes	no	yes	no	no	no	T18_C05_50_1L_US
T23	20	no	yes	no	no	no	no	no	T23_C05_20_1L_US
T23_1	20	yes	yes	no	yes	no	no	no	T23_1_C05_20_1L_US
T27	30	yes	yes	yes	no	yes	no	no	T27_C05_30_1L_US

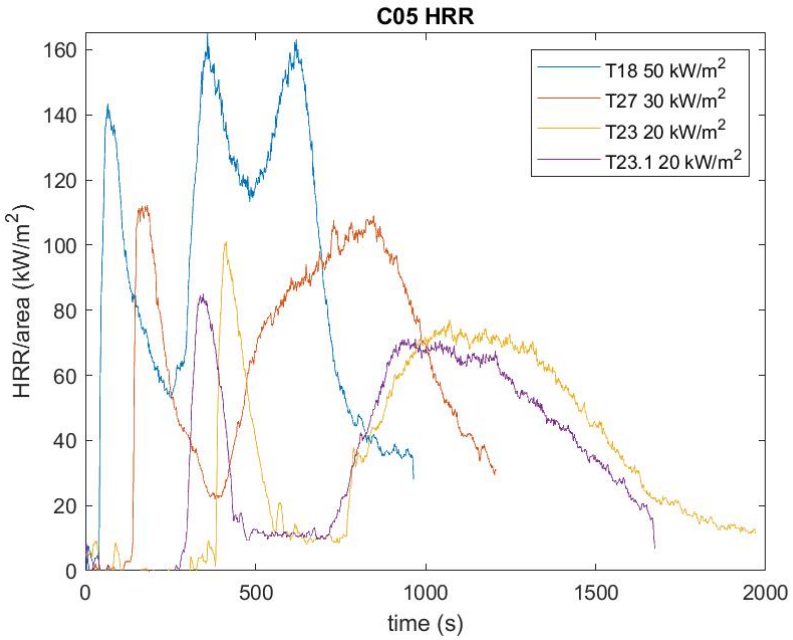

Figure 21. Heat release rates per unit area of Cable 5 at different heat fluxes.

Cable 5 was tested four times at three different heat flux levels as presented in Figure 21. The graphs show a bimodal behaviour as first the sheath of the cable is ignited and then the insulation material of the conductors is ignited which results in some variation in the second peak. T23 was performed twice (T23 and T23.1) due to a malfunction of DMS equipment in T23. This did not affect the HRR measurement, but the repeated test shows that repeatability between to similar tests may differ. This can be caused by the sample preparation in arranging the cables in the sample holder prior to the tests. In some tests it was seen that the cables were bent during combustion. Both tests, T23 and T23.1, were reignited with igniter inserted after flameout after the first peak.

The following graphs, Figure 22 and Figure 23, show the mass loss rates and obscuration at the tests.

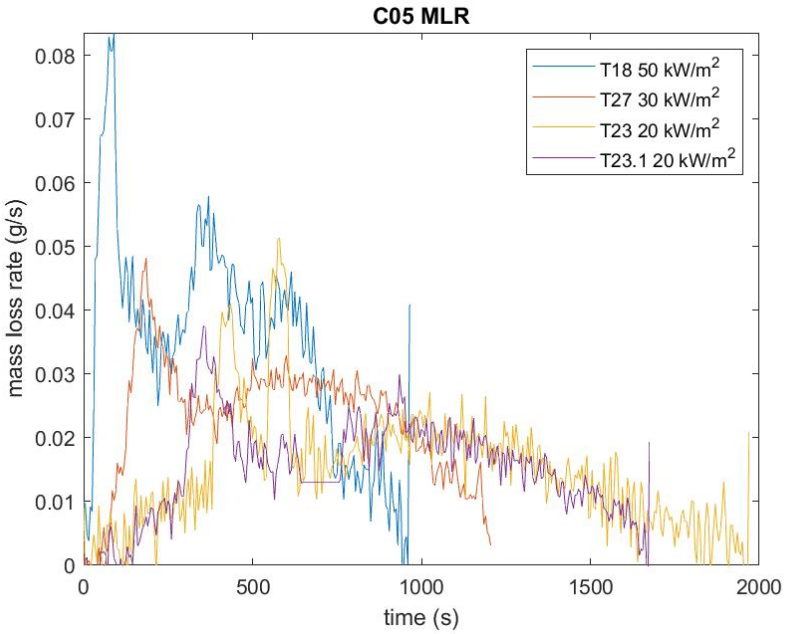

Figure 22. Mass loss rate of Cable 5 at different heat fluxes.

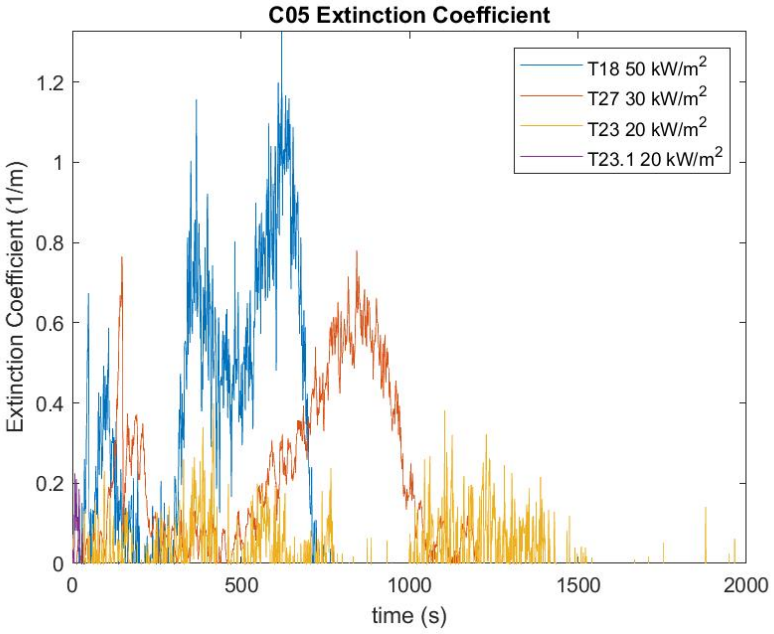

Figure 23. Obscuration of Cable 5 at different heat fluxes.

Figure 24 shows the time dependent values of heat of combustion during each test.

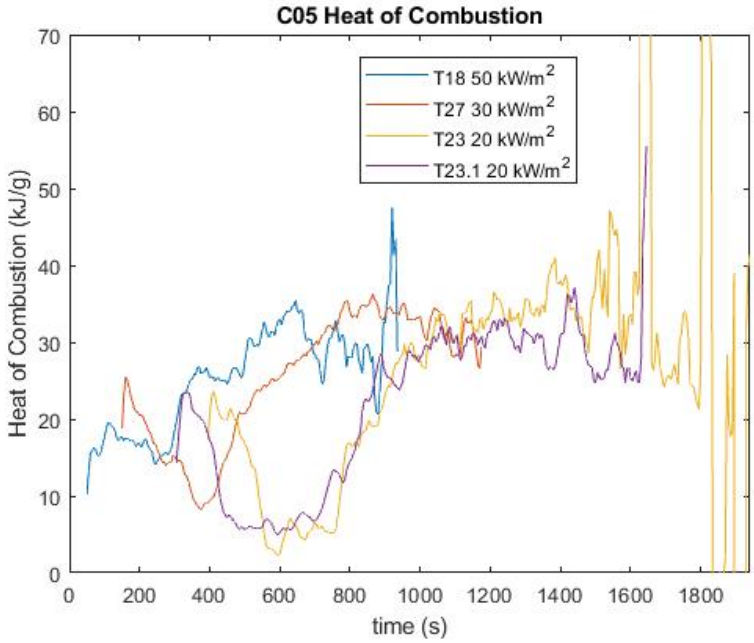

Figure 24. Heat of Combustion from ignition to 30 seconds before end of test.

In Table 10, the resulting fire properties are presented for each test. The yields and heat of combustion are calculated as average values for the test. For T23 and T23.1, it should be noted that the samples were extinguished between the combustion of the sheath and insulation material of the conductors. This intermittent burning process affects the yields and heat of combustion as the burning process were interrupted.

Table 10. Fire properties of Cable 5 at different heat fluxes.

Test	Heat flux [kW/m2]	Time to ignition [s]	CO2-yield [kg/kg]	CO-yield [kg/kg]	Heat of Combustion [MJ/kg]
T18	50	47	1.54	0.026	22.80
T23	20	392	1.42	0.060	21.67
T23.1	20	302	1.51	0.057	21.73
T27	30	148	1.69	0.035	24.63

2.6 Cable 6, C06

Cable 6 is a white multi conductor cable with an outer diameter of 15 mm. The sales marking is CAB.SIG.BL.13x2x0.50mm2 NE26. The cable was tested in the cone calorimeter in a single test according to Table 11.

Table 11. Performed tests of Cable 6, C06.

Test	Heat flux [kW/m^2]	DMS	Aethalo-meter	DGI	APM	TEM	ICP-MS	VAC	File name
T44	50	yes	yes	no	no	no	no	no	T44_C06_50_1L_US

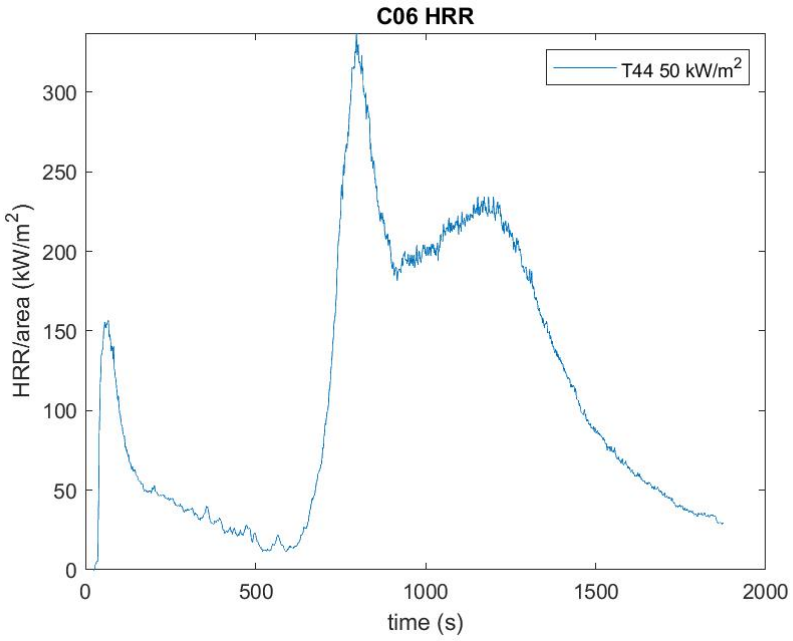

Figure 25. Heat release rates per unit area of Cable 6 at 50 kW/m^2 heat flux.

Cable 6 was tested in a single test at 50 kW/m^2 heat flux as presented in Figure 25. The graph show a bimodal behaviour as first the sheath of the cable is ignited and then the insulation material of the conductors is ignited which results in some variation in the second peak. The sample was extinguished after the combustion of the sheath. So, the igniter was inserted for the second ignition which resulted in the second peak.

The following graphs, Figure 26 and Figure 27, show the mass loss rates and obscuration at the tests.

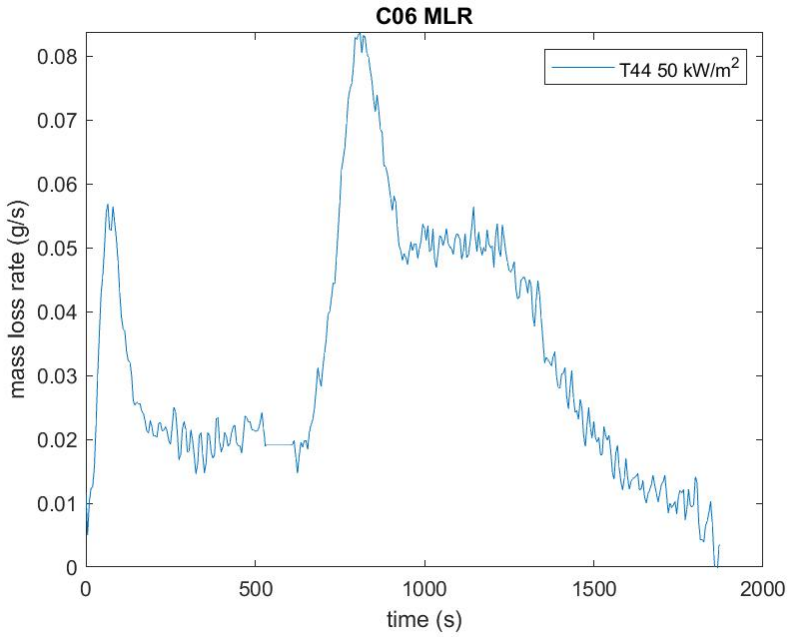

Figure 26. Mass loss rate of Cable 6 at 50 kW/m^2 heat flux.

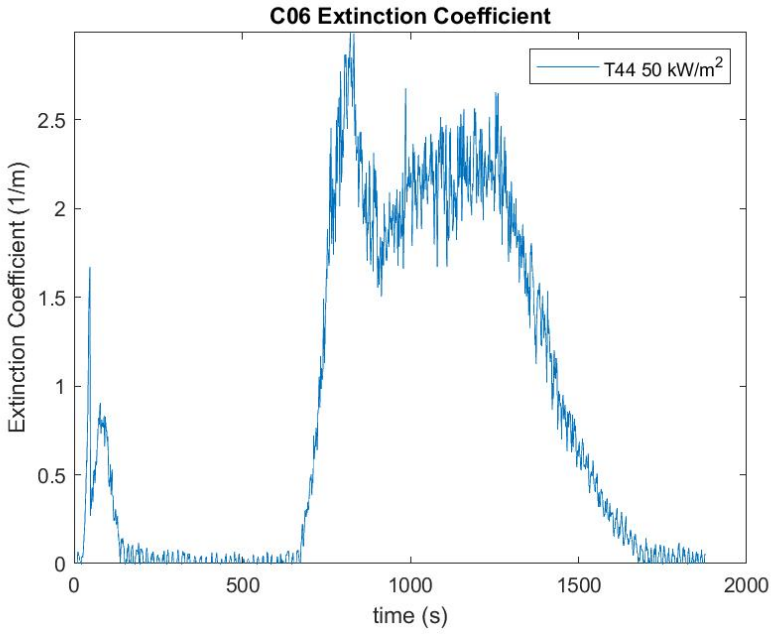

Figure 27. Obscuration of Cable 6 at different heat fluxes.

Figure 28 shows the time dependent values of the heat of combustion during T44.

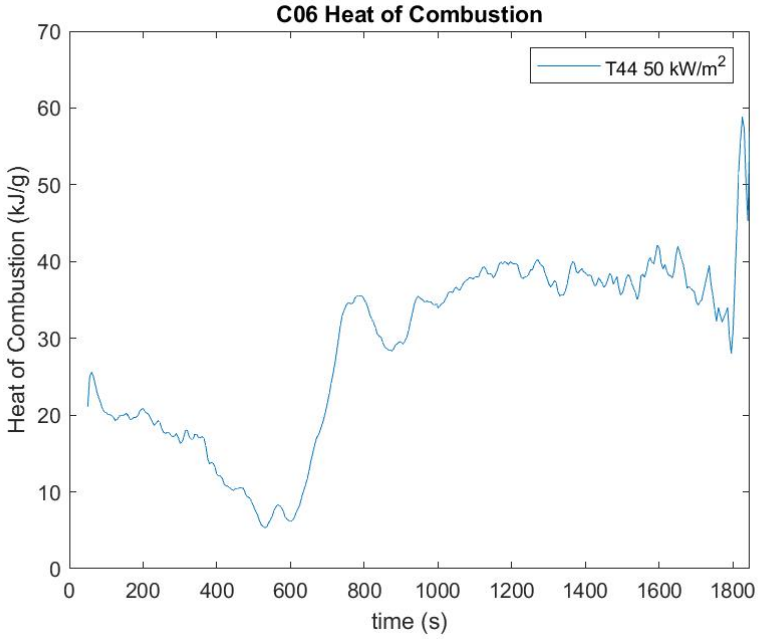

Figure 28. Heat of Combustion from ignition to 30 seconds before end of test.

In Table 12, the resulting fire properties are presented for T44. The yields and heat of combustion are calculated as average values for the test. It should be noted that the sample was extinguished between the combustion of the sheath and insulation material of the conductors. This intermittent burning process affects the yields and heat of combustion as the burning process were interrupted.

Table 12. Fire properties of Cable 6 at 50 kW/m² heat flux.

Test	Heat flux [kW/m2]	Time to ignition [s]	CO2-yield [kg/kg]	CO-yield [kg/kg]	Heat of Combustion [MJ/kg]
T44	50	49	1.94	0.045	29.85

2.7 Cable 7, C07

Cable 7 is a white multi conductor cable with an outer diameter of 19 mm. The sales marking is CAB.SIG.BL.24x2x0.50mm2 NE48. The cable was tested in three tests according to Table 13.

Table 13. Performed tests of Cable 7, C07.

Test	Heat flux [kW/m^2]	DMS	Aethalo-meter	DGI	APM	TEM	ICP-MS	VAC	File name
T8	20	yes	yes	no	no	no	no	no	T8_C07_20_1L_US
T10	30	yes	yes	no	yes	no	no	no	T10_C07_30_1L_US
T45	50	yes	yes	no	no	no	no	no	T45_C07_50_1L_US

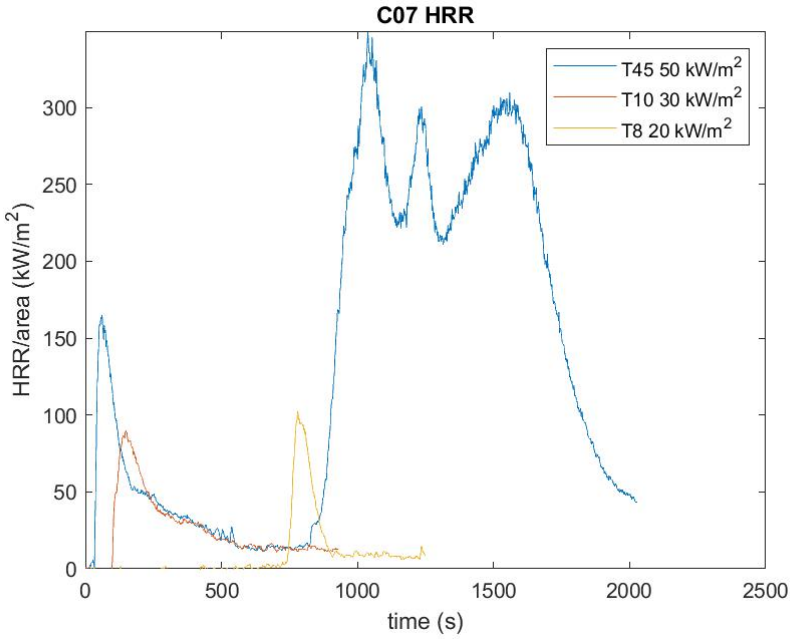

Figure 29. Heat release rates per unit area of Cable 7 at different heat fluxes.

Cable 7 was tested three times at three different heat flux levels as presented in Figure 29. The graph of T45 show a bimodal behaviour as first the sheath of the cable is ignited and then the insulation material of the conductors is ignited which results in some variation in the second peak in T45. In T8 and T10, the incident heat flux was not enough to ignite the insulation material of the conductors. For all three tests, the igniter was inserted after the extinction after the first peak.

The following graphs, Figure 30 and Figure 31, show the mass loss rates and obscuration for the tests.

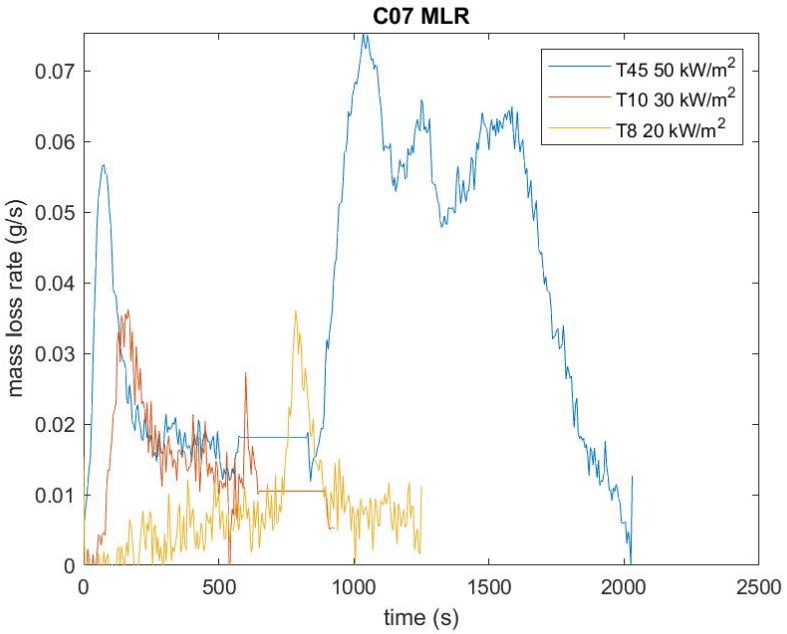

Figure 30. Mass loss rate of Cable 7 at different heat fluxes.

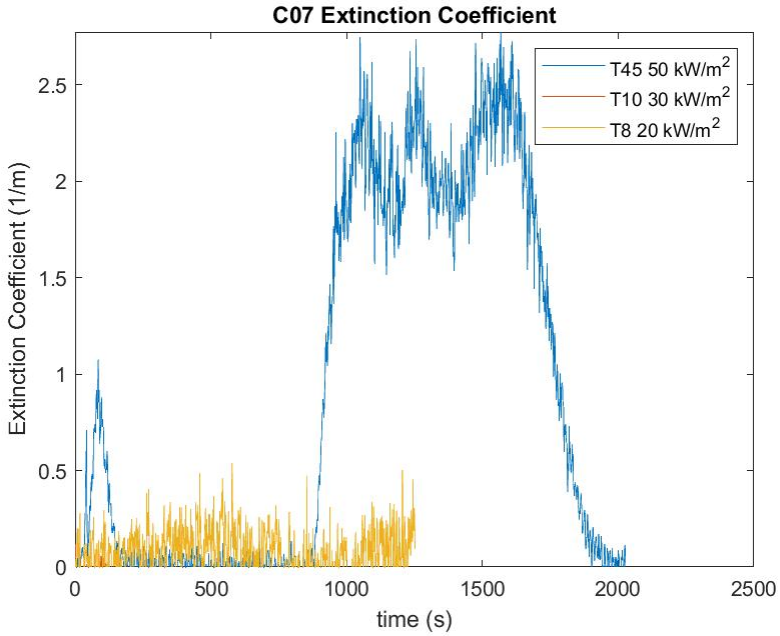

Figure 31. Obscuration of Cable 7 at different heat fluxes.

Figure 32 shows the time dependent values of heat of combustion during each test.

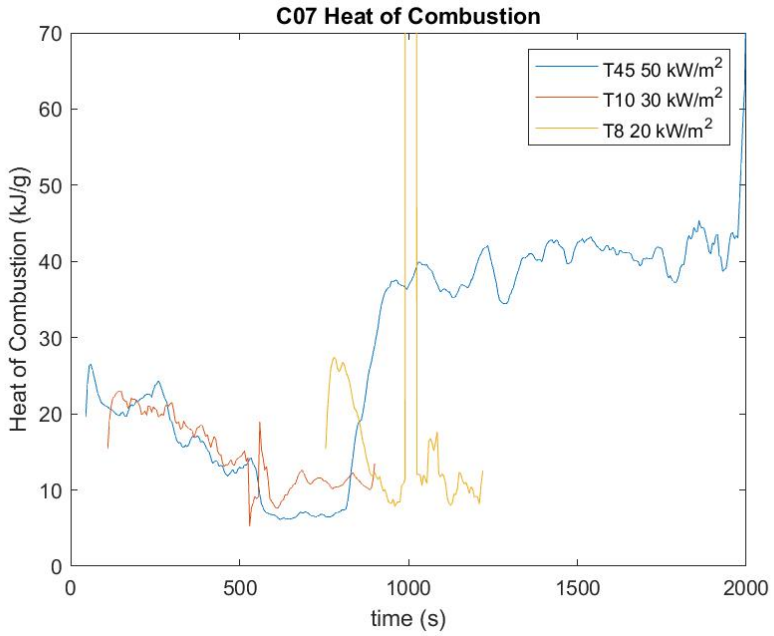

Figure 32. Heat of Combustion from ignition to 30 seconds before end of test.

In Table 14, the resulting fire properties are presented for each test. The yields and heat of combustion are calculated as average values for the test. For all three tests it should be noted that the samples were extinguished after the first combustion of the sheath. In T45, the sample was reignited but in T10 and T45 the tests were stopped after a period of pyrolysis without ignition of the insulation material of the conductors. This intermittent burning process affects the yields and heat of combustion as the burning process were interrupted.

Table 14. Fire properties of Cable 7 at different heat fluxes.

Test	Heat flux [kW/m2]	Time to ignition [s]	CO2-yield [kg/kg]	CO-yield [kg/kg]	Heat of Combustion [MJ/kg]
T8	20	751	1.21	0.106	17.25
T10	30	105	0.96	0.085	15.67
T45	50	43	2.10	0.043	33.33

2.8 Cable 8, C08

Cable 8 is an orange multi conductor cable with an outer diameter of 9,5 mm. The sales marking is CABLE ANTIFEU 2x1.5mm² MHF2. The cable was tested in three tests according to Table 15.

Table 15. Performed tests of Cable 8, C08.

Test	Heat flux [kW/m2]	DMS	Aethalo-meter	DGI	APM	TEM	ICP-MS	VAC	File name
T6	20	yes	yes	no	no	no	no	no	T6_C08_20_1L_US
T11	30	yes	yes	no	yes	no	no	no	T11_C08_30_1L_US
T46	50	yes	yes	no	no	no	no	no	T46_C08_50_1L_US

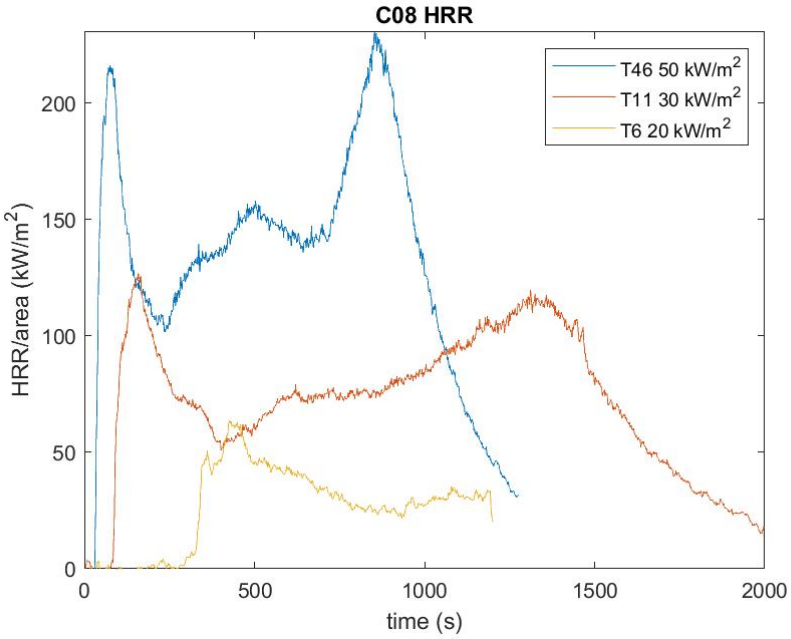

Figure 33. Heat release rates per unit area of Cable 8 at different heat fluxes.

Cable 8 was tested at three different heat flux levels as presented in Figure 33. The graphs, T11 and T46, show a bimodal behaviour as first the sheath of the cable is ignited and then insulation material of the conductors is ignited. In T6, the sheath was ignited but the incident heat flux was not enough to ignite the insulation material of the conductors. Small flames were present at end of T6.

The following graphs, Figure 34 and Figure 35, show the mass loss rates and obscuration at the tests.

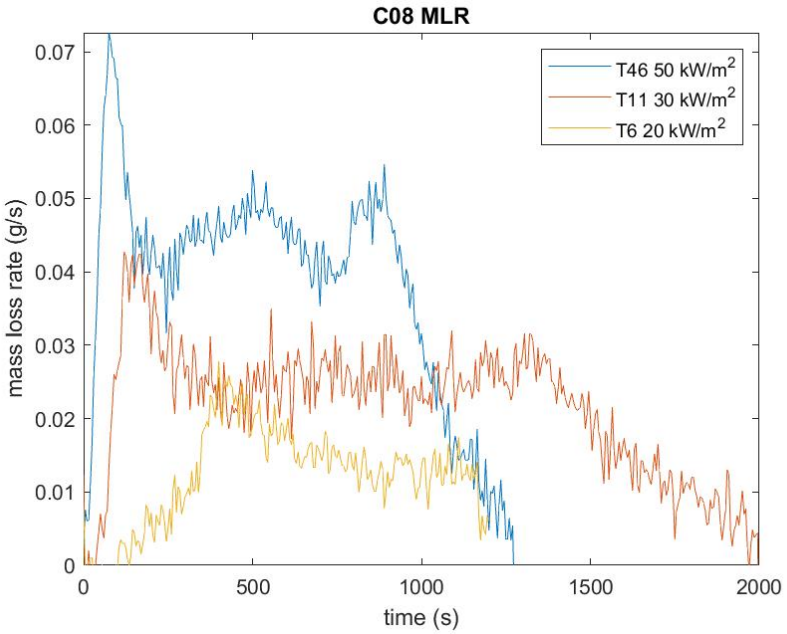

Figure 34. Mass loss rate of Cable 8 at different heat fluxes.

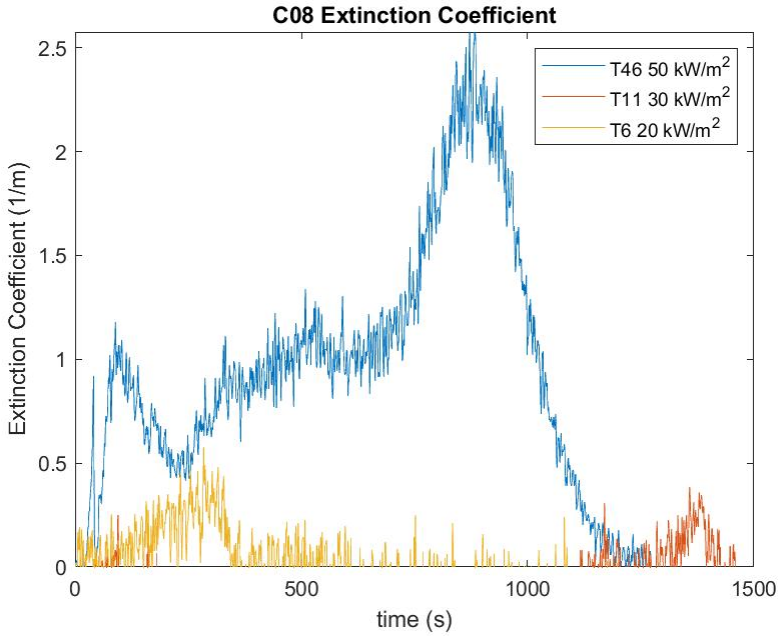

Figure 35. Obscuration of Cable 8 at different heat fluxes.

Figure 36 shows the time dependent values of heat of combustion during each test.

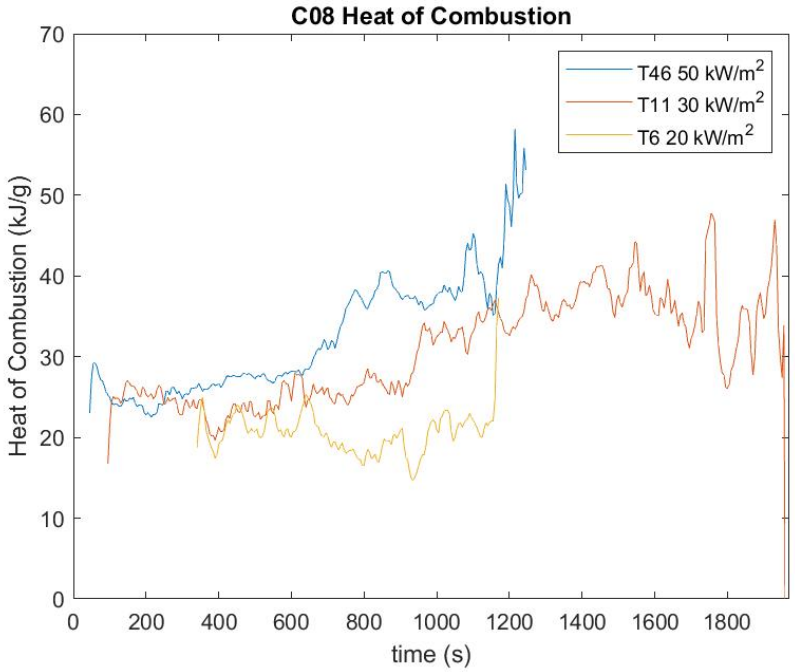

Figure 36. Heat of Combustion from ignition to 30 seconds before end of test.

In Table 16, the resulting fire properties are presented for each test. The yields and heat of combustion are calculated as average values for the test. In T6, the test was stopped after a period of pyrolysis and some small flames at the edges. This burning process without flaming combustion over the whole sample surface affects the yields and heat of combustion.

Table 16. Fire properties of Cable 8 at different heat fluxes.

Test	Heat flux [kW/m2]	Time to ignition [s]	CO2-yield [kg/kg]	CO-yield [kg/kg]	Heat of Combustion [MJ/kg]
T6	20	337	1.44	0.077	20.69
T11	30	94	2.03	0.024	29.30
T46	50	40	1.93	0.027	30.08

2.9 Cable 9, C09

Cable 9 is an orange multi conductor cable with an outer diameter of 34.5 mm. The sales marking is CAB.SIG.BL. 24x2x1.5mm² NHF48. The cable was tested in three tests according to Table 17.

Table 17. Performed tests of Cable 9, C09.

Test	Heat flux [kW/m2]	DMS	Aethalo-meter	DGI	APM	TEM	ICP-MS	VAC	File name
T7	20	yes	yes	no	no	no	no	no	T7_C09_20_1L_US
T12	30	yes	yes	no	yes	no	no	no	T12_C09_30_1L_US
T13	50	yes	yes	no	yes	no	no	no	T13_C09_50_1L_US

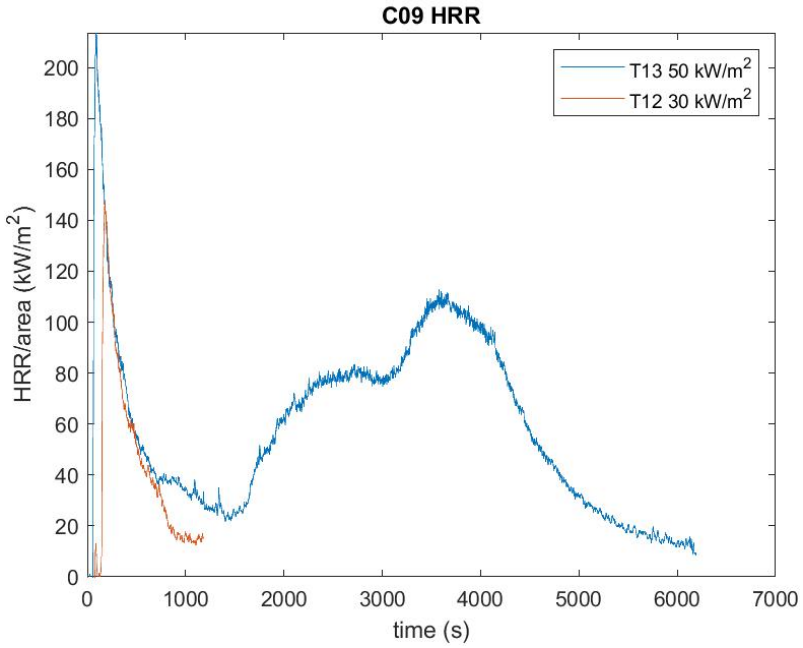

Figure 37. Heat release rates per unit area of Cable 9 at different heat fluxes.

Cable 9 was tested at two different heat flux levels as presented in Figure 37. T13 shows a bimodal behaviour as first the sheath of the cable is ignited and then insulation material of the conductors is ignited. As the cable has a large diameter, the cable consists of a thick sheath and a large mass of insulation materials which leads to a long burning time. The single peak T12 derives from ignition of the sheath but the insulation material of the conductors is not ignited (igniter reinserted) within the time frame of the test. The sample in T7 was not ignited at all due to a low incident heat flux.

The following graphs, Figure 38 and Figure 39, show the mass loss rates and obscuration at the tests.

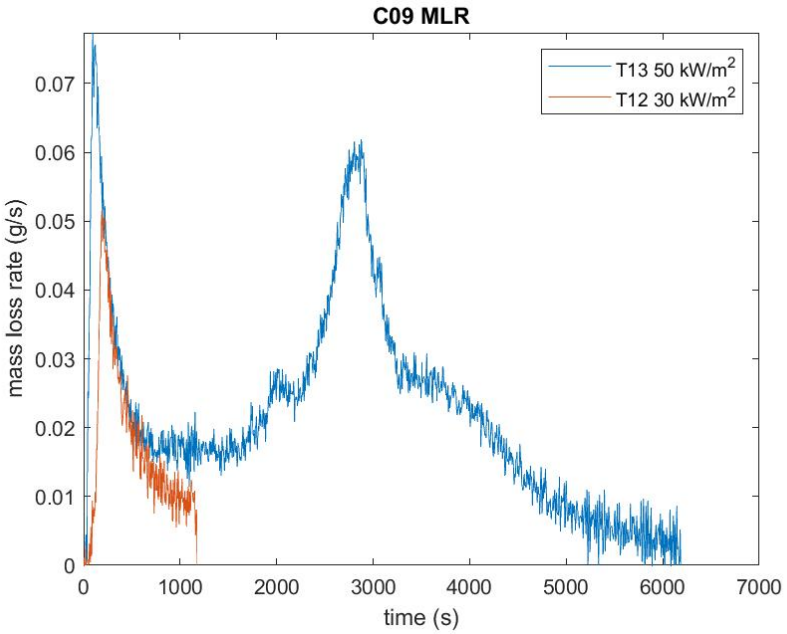

Figure 38. Mass loss rate of Cable 9 at different heat fluxes.

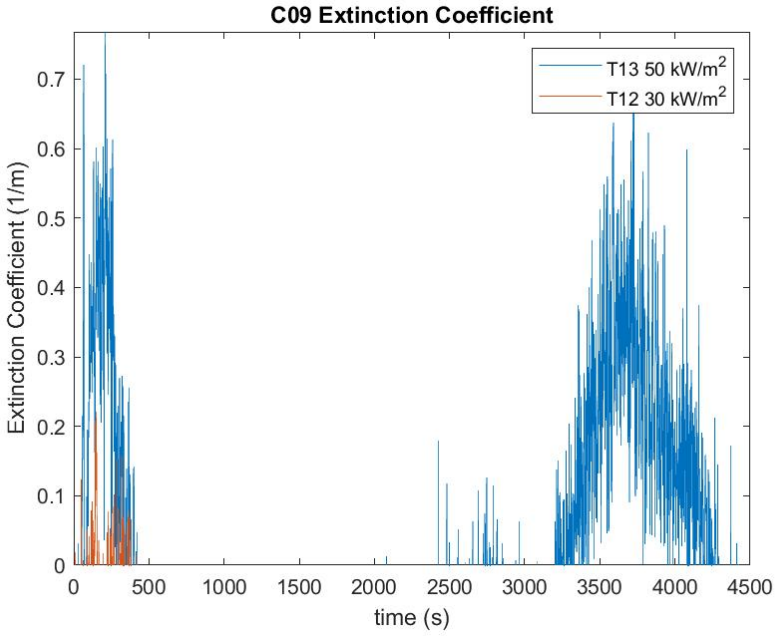

Figure 39. Obscuration of Cable 9 at different heat fluxes.

Figure 40 shows the time dependent values of heat of combustion during each test.

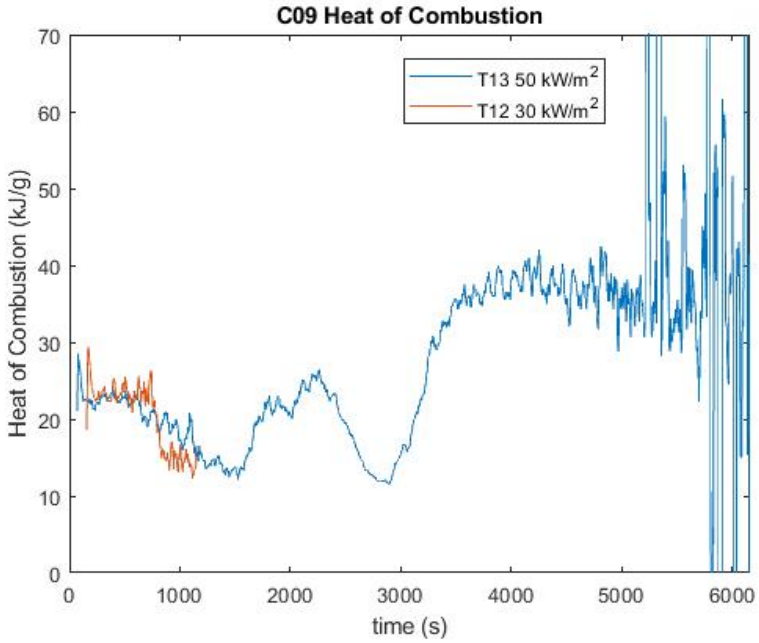

Figure 40. Heat of Combustion from ignition to 30 seconds before end of test.

In Table 18, the resulting fire properties are presented for each test. The yields and heat of combustion are calculated as average values for the test. In T12, the test was stopped after a period of pyrolysis without ignition. This burning process affects the yields and heat of combustion.

Table 18. Fire properties of Cable 9 at different heat fluxes.

Test	Heat flux [kW/m2]	Time to ignition [s]	CO2-yield [kg/kg]	CO-yield [kg/kg]	Heat of Combustion [MJ/kg]
T7	20	No ignition	-	-	-
T12	30	94	1.46	0.067	21.57
T13	50	152	1.59	0.038	23.74

2.10 Cable 10, C10

Cable 10 is an orange multi conductor cable with an outer diameter of 7.5 mm. The sales marking is CAB.SIG.BL. 1x2x0.75mm² NFF2. The cable was tested in four tests according to Table 19.

Table 19. Performed tests of Cable 10, C10.

Test	Heat flux [kW/m2]	DMS	Aethalo-meter	DGI	APM	TEM	ICP-MS	VAC	File name
T3	50	yes	yes	no	yes	no	no	no	T3_C10_50_1L_US
T9	30	yes	yes	no	yes	no	no	no	T9_C10_30_1L_US
T14	50	yes	yes	no	yes	no	no	no	T14_C10_50_1L_US
T47	20	yes	yes	no	no	no	no	no	T47_C10_20_1L_US

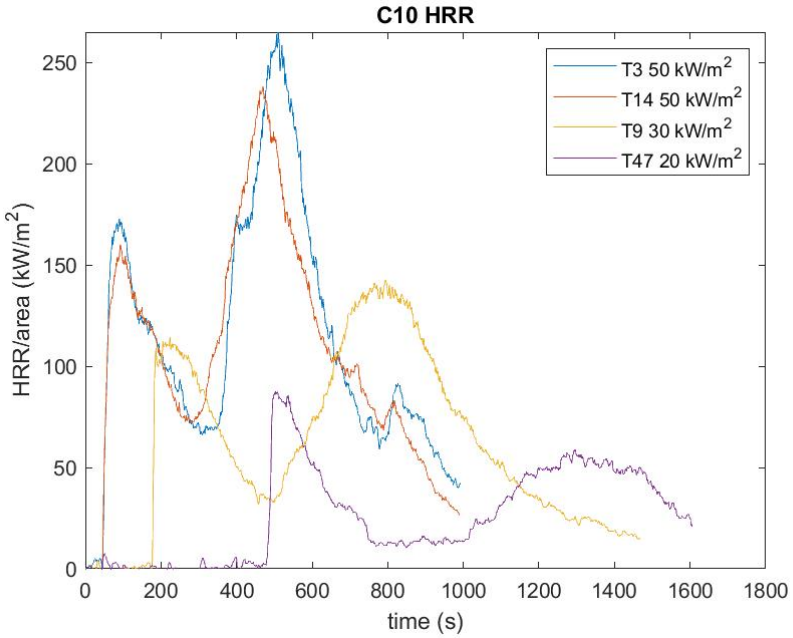

Figure 41. Heat release rates per unit area of Cable 10 at different heat fluxes.

Cable 10 was tested four times at three different heat flux levels as presented in Figure 41. The graphs shows a bimodal behaviour as first the sheath of the cable is ignited and then insulation material of the conductors is ignited. In T47, the sample was extinguished after 754 seconds. The igniter was then inserted followed by a period of flashing and reignition at 1021 seconds.

The following graphs, Figure 42 and Figure 43, show the mass loss rates and obscuration at the tests.

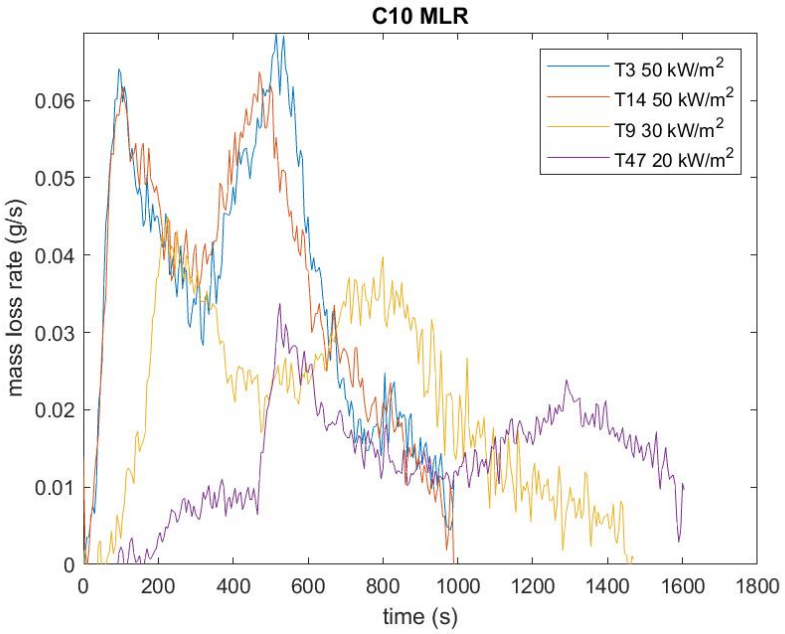

Figure 42. Mass loss rate of Cable 10 at different heat fluxes.

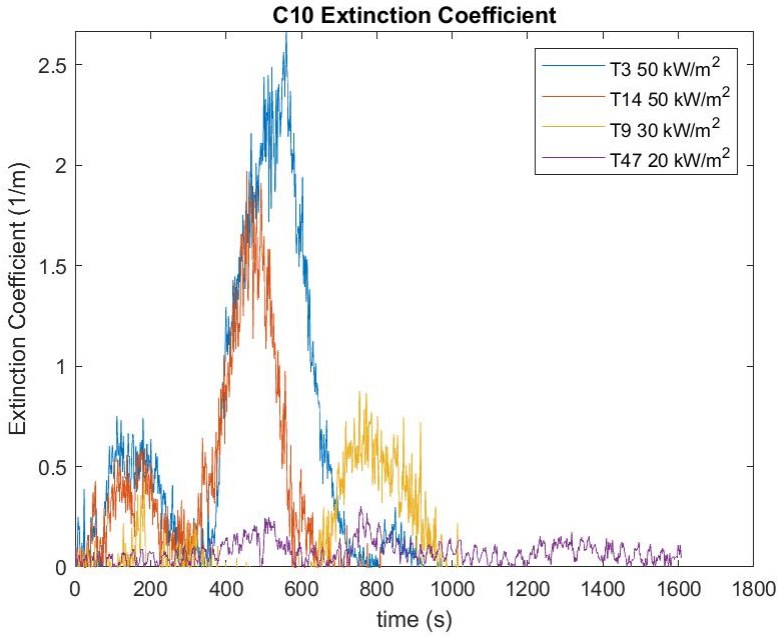

Figure 43. Obscuration of Cable 10 at different heat fluxes.

Figure 44 shows the time dependent values of heat of combustion during each test.

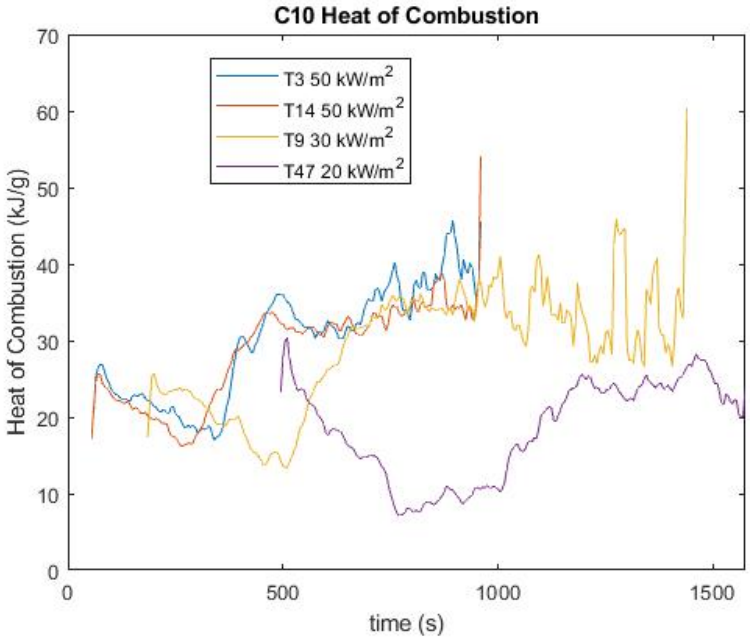

Figure 44. Heat of Combustion from ignition to 30 seconds before end of test.

In Table 20, the resulting fire properties are presented for each test. The yields and heat of combustion are calculated as average values for the test. It should be noted that the sample in T47 was extinguished between the combustion of the sheath and insulation material of the conductors. This intermittent burning process affects the yields and heat of combustion as the burning process were interrupted.

Table 20. Fire properties of Cable 10 at different heat fluxes.

Test	Heat flux [kW/m2]	Time to ignition [s]	CO2-yield [kg/kg]	CO-yield [kg/kg]	Heat of Combustion [MJ/kg]
T3	50	55	1.95	0.031	28.34
T9	30	184	1.87	0.038	27.01
T14	50	53	1.86	0.029	27.51
T47	20	491	1.25	0.067	18.92

2.11 Cable 11, C11

Cable 11 is a black single conductor cable with an outer diameter of 23 mm. The cable consists of a sheath, insulation material and a core of wires. The sales marking is FLEX.COPPER CABLE 150 mm^2. The cable was tested in two tests according to Table 21.

Table 21. Performed tests of Cable 11, C11.

Test	Heat flux [kW/m2]	DMS	Aethalo-meter	DGI	APM	TEM	ICP-MS	VAC	File name
T48	30	yes	yes	no	no	no	no	no	T48_C11_30_1L_US
T50	50	yes	yes	no	no	no	no	no	T50_C11_50_1L_US

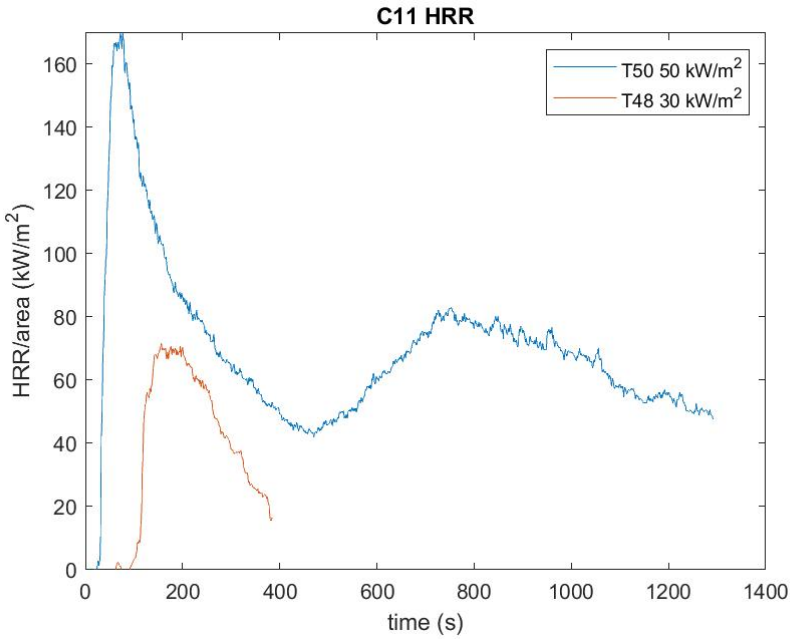

Figure 45. Heat release rates per unit area of Cable 11 at different heat fluxes.

Cable 11 was tested at two different heat flux levels as presented in Figure 45. T50 shows a bimodal behaviour as first the sheath of the cable is ignited and then the insulation material is ignited. The single peak at 30 kW/m^2 derives from combustion of the sheath but the insulation material of the interior cable was not ignited within the time frame of the test.

The following graphs, Figure 46 and Figure 47, show the mass loss rates and obscuration at the tests.

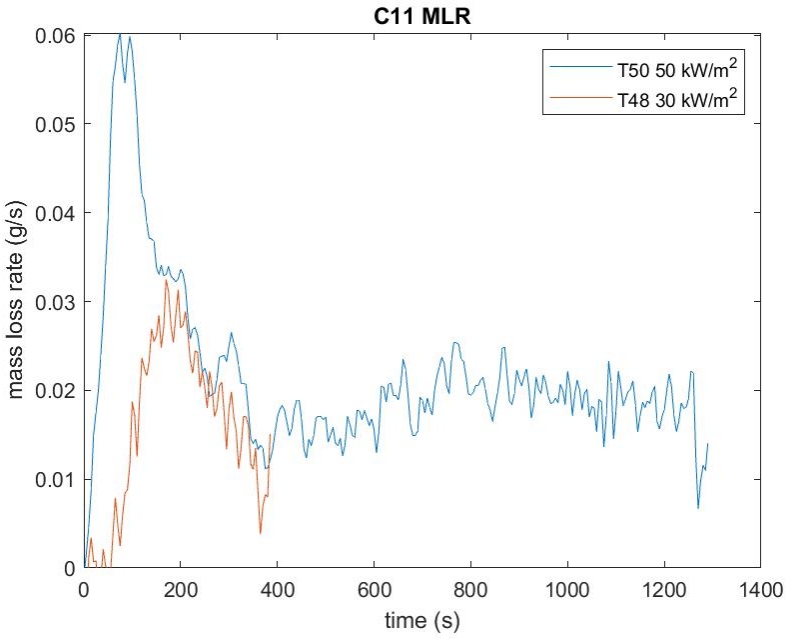

Figure 46. Mass loss rate of Cable 11 at different heat fluxes.

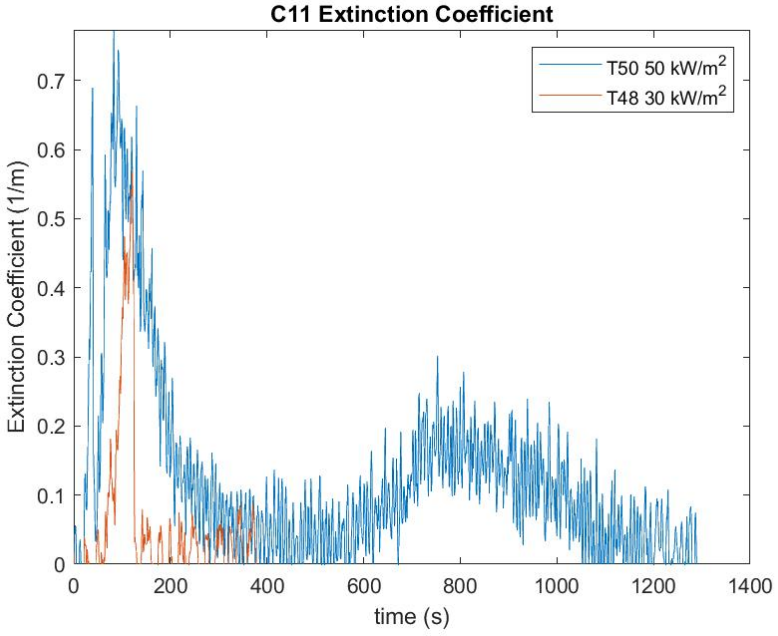

Figure 47. Obscuration of Cable 11 at different heat fluxes.

Figure 48 shows the time dependent values of heat of combustion during each test.

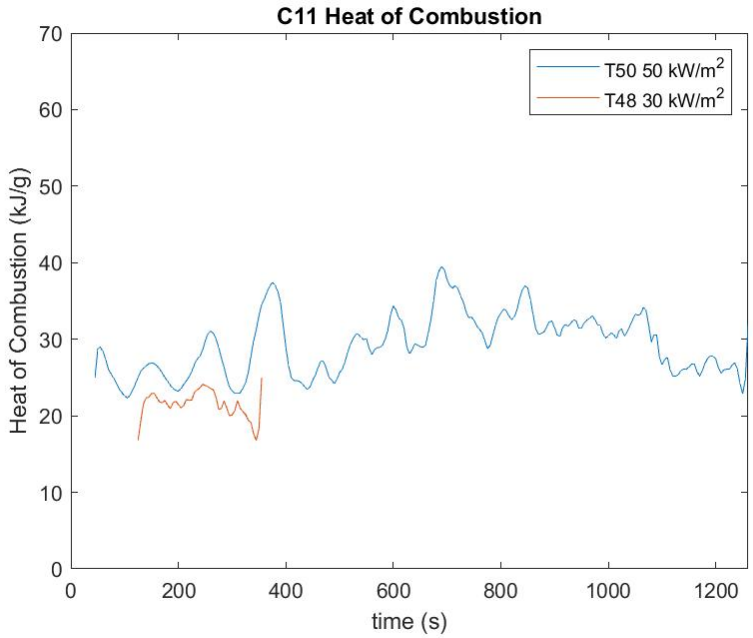

Figure 48. Heat of Combustion from ignition to 30 seconds before end of test.

In Table 22, the resulting fire properties are presented for each test. The yields and heat of combustion are calculated as average values for the test. In T48, the test was stopped after a period of pyrolysis without ignition. This burning process affects the yields and heat of combustion.

Table 22. Fire properties of Cable 11 at different heat fluxes.

Test	Heat flux [kW/m2]	Time to ignition [s]	CO2-yield [kg/kg]	CO-yield [kg/kg]	Heat of Combustion [MJ/kg]
T48	30	122	1.32	0.052	19.59
T50	50	44	1.86	0.031	28.03

2.12 Cable 12, C12

Cable 12 is a black multi conductor cable with an outer diameter of 22 mm. The sales marking is CABLE Cu FLEX. 5x16mm ² PN5SJ. The cable was tested in two tests according to Table 23.

Table 23. Performed tests of Cable 12, C12.

Test	HEAT FLUX [kW/m2]	DMS	Aethalo-meter	DGI	APM	TEM	ICP-MS	VAC	File name
T49	30	yes	yes	no	no	no	no	no	T49_C12_30_1L_US
T51	50	yes	yes	no	no	no	no	no	T51_C12_50_1L_US

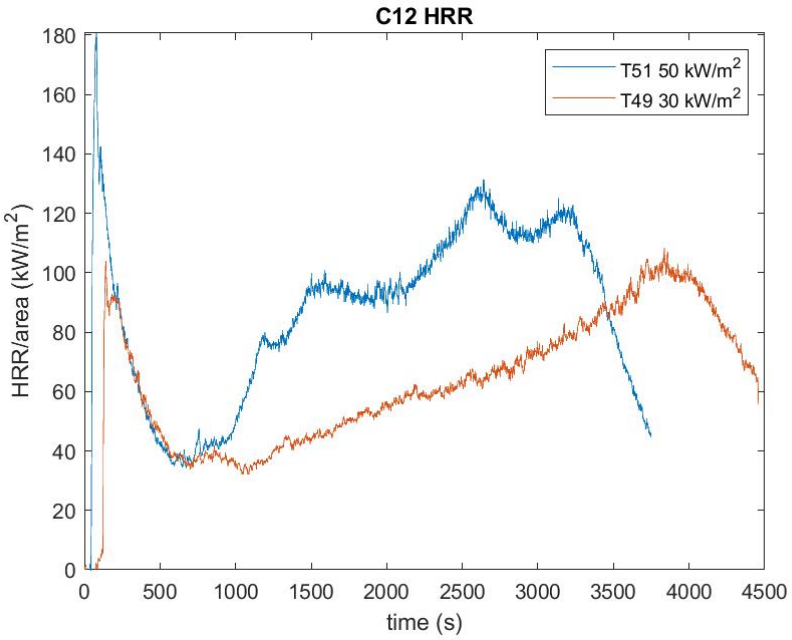

Figure 49. Heat release rates per unit area of Cable 12 at different heat fluxes.

Cable 12 was tested at two different heat flux levels as presented in Figure 49. The figures show a bimodal behaviour as first the sheath of the cable is ignited and then insulation material of the conductors is ignited.

The following figures, Figure 50 and Figure 51, show the mass loss rates and obscuration for the tests.

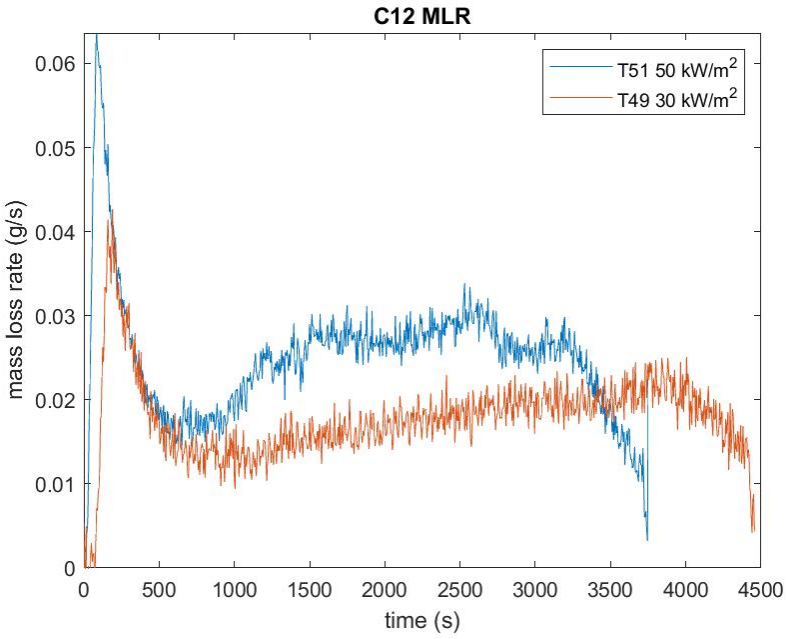

Figure 50. Mass loss rate of Cable 12 at different heat fluxes.

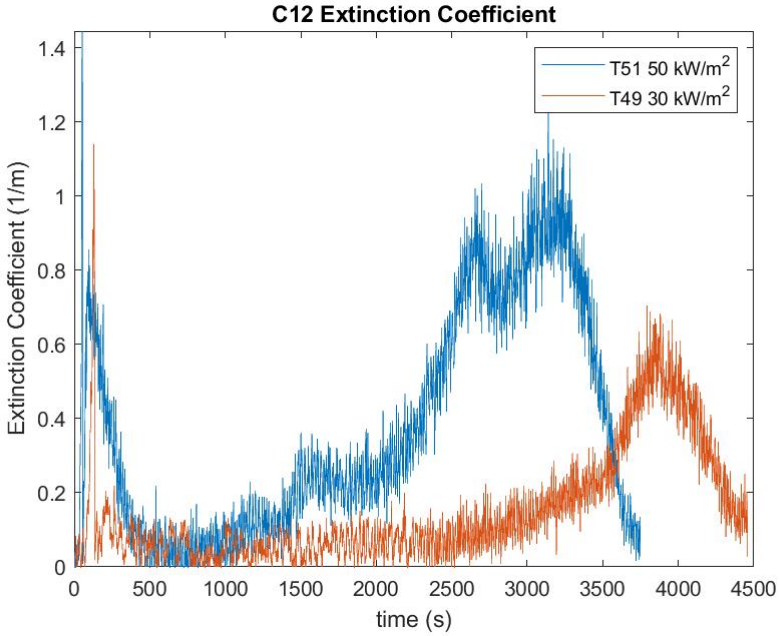

Figure 51. Obscuration of Cable 12 at different heat fluxes.

Figure 52 shows the time dependent values of heat of combustion during each test.

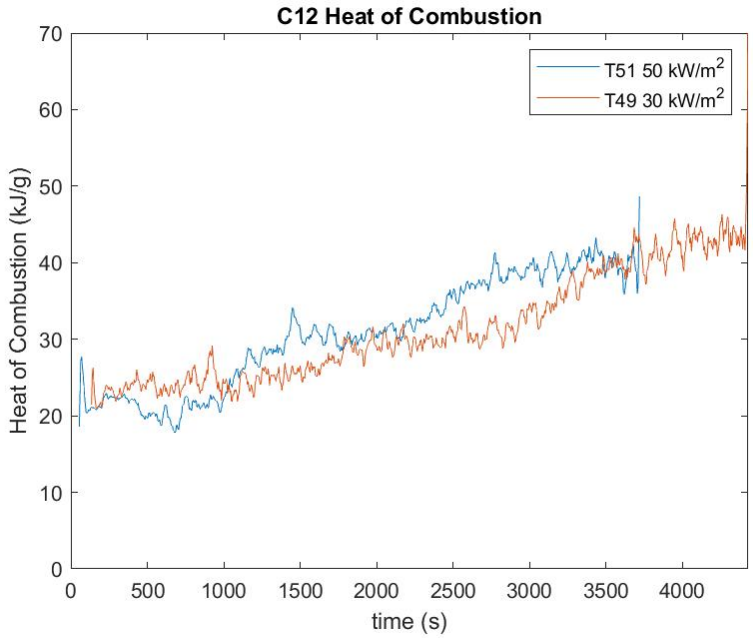

Figure 52. Heat of Combustion from ignition to 30 seconds before end of test.

In Table 24, the resulting fire properties are presented for each test. The yields and heat of combustion are calculated as average values for the test. Both tests had a period of low intensity burning before the combustion of the insulation materials of the conductors. In T49, this period was a bit longer, which may have affected the CO-yield.

Table 24. Fire properties of Cable 12 at different heat fluxes.

Test	Heat flux [kW/m2]	Time to ignition [s]	CO2-yield [kg/kg]	CO-yield [kg/kg]	Heat of Combustion [MJ/kg]
T49	30	132	2.10	0.055	31.43
T51	50	53	2.12	0.023	30.58

2.13 Electrical boards, E01-E04

Electrical boards come from old EPC recup service. The electrical boards consisted of a base plate with varying electrical components mounted. Each board was tested in a single test as presented in Table 25.

Table 25. Performed test of E01-E04.

Board	Test	Heat flux [kW/m2]	DMS	Aethalo-meter	DGI	APM	TEM	ICP-MS	VAC	File name
E01	T31	20	yes	Yes	yes	yes	no	no	no	T31_E01_20_1L_US
E02	T32	30	yes	yes	no	no	no	no	no	T32_E02_30_1L_US
E03	T33	20	yes	yes	no	no	no	no	no	T33_E03_20_1L_US
E04	T34	50	yes	yes	no	no	no	no	no	T34_E04_50_1L_US

Figure 53. T31, E01 in sample holder.

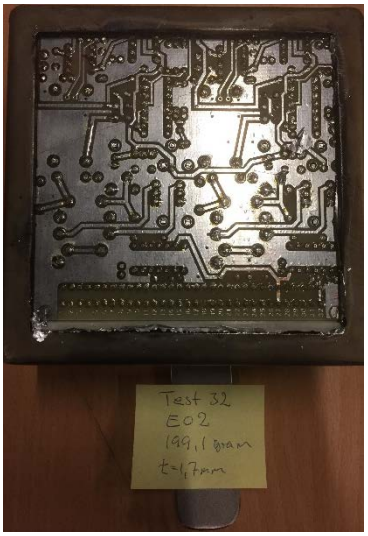

Figure 54. T32, E02 in sample holder.

Figure 56. T33, E03 in sample holder.

Figure 55. T34, E04 in sample holder.

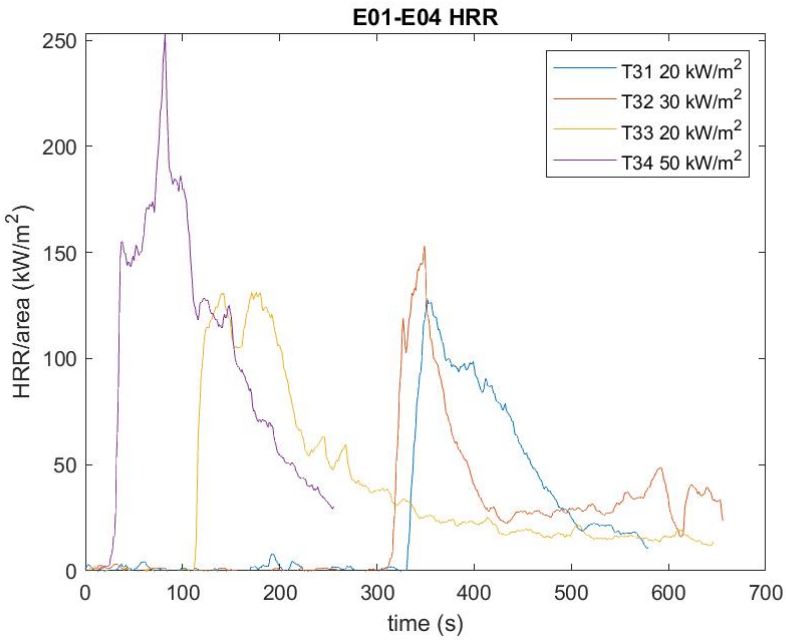

Figure 57. Heat release rates per unit area of Electrical boards, E01-EO4, at different heat fluxes.

The electrical boards were tested in single tests and resulted mostly in a single peak of the plastic base plate as presented in Figure 57. In T34, a distinct smell was developed, escaping the ventilation.

The following graphs, Figure 58 and Figure 59, show the mass loss rates and obscuration at the tests.

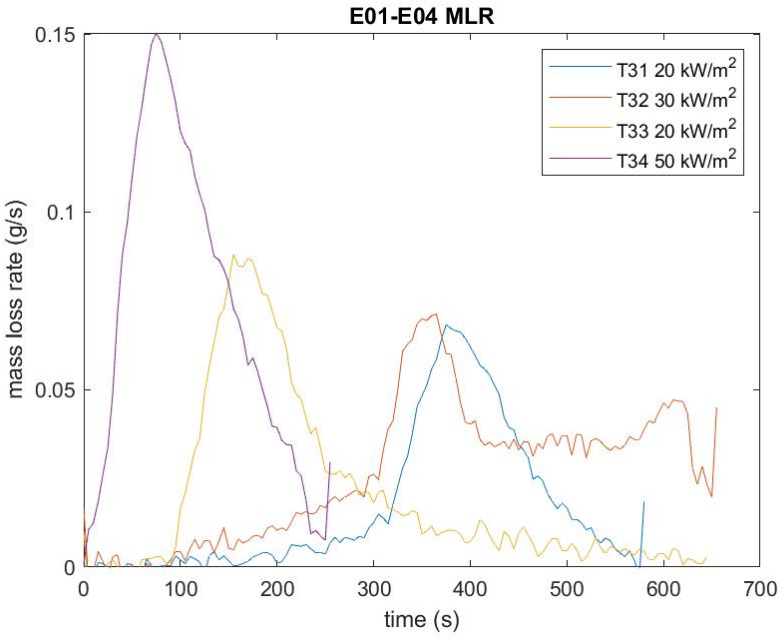

Figure 58. Mass loss rate of Electrical boards, E01-E04, at different heat fluxes.

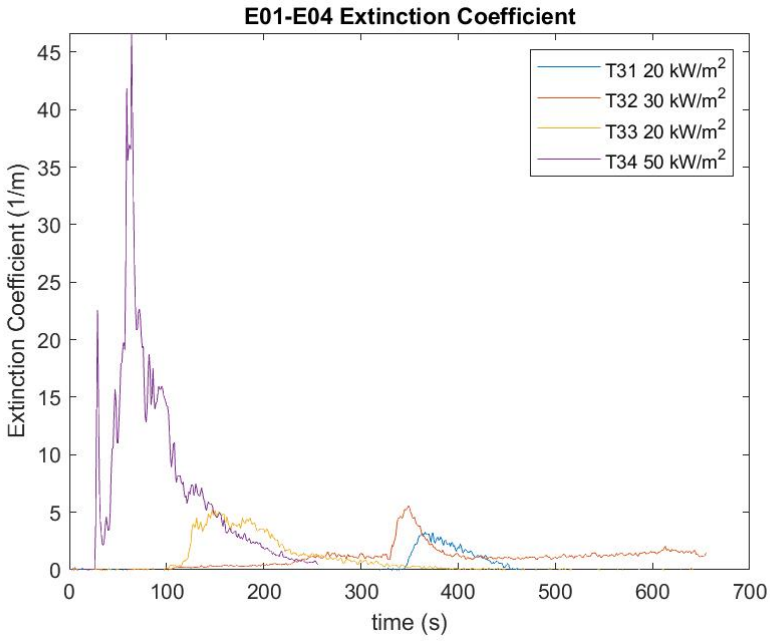

Figure 59. Obscuration of Electrical boards, E01-E04, at different heat fluxes.

Figure 60 shows the time dependent values of heat of combustion during each test.

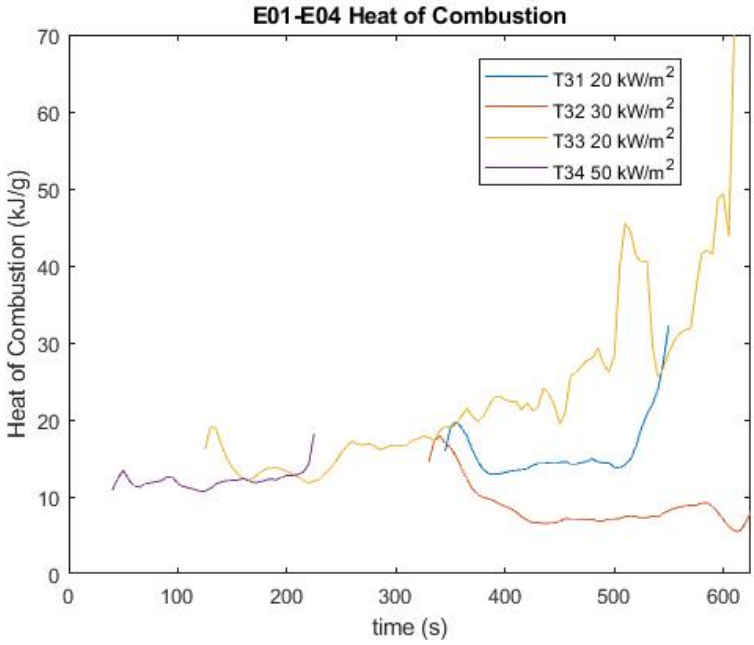

Figure 60. Heat of Combustion from ignition to 30 seconds before end of test.

In Table 26, the resulting fire properties are presented for each test. The yields and heat of combustion are calculated as average values for the test.

Table 26. Fire properties of Electrical boards, E01-E04, at different heat fluxes.

Board	Test	Heat flux [kW/m2]	Time to ignition [s]	CO2-yield [kg/kg]	CO-yield [kg/kg]	Heat of Combustion [MJ/kg]
E01	T31	20	340	1.09	0.069	13.68
E02	T32	30	327	0.57	0.116	9.11
E03	T33	20	121	0.91	0.114	15.41
E04	T34	50	39	0.74	0.133	11.57

2.14 Materials, M01-M02

Material M01, is a plastic sheet and used to isolate magnets. The sales marking is STRAT.GLASS FABR.SHEET E 2. Material M02, is a SPS magnetic coil with a combustible plastic insulation material. The materials were tested in two tests for M01 and a single test for M02 as presented in Table 27.

Table 27. Performed tests of M01.

Material	Test	Heat flux [kW/m²]	DMS	Aethalo-meter	DGI	APM	TEM	ICP-MS	VAC	File name
M01	T28	30	yes	yes	yes	No	no	no	no	T28_M01_30_1L_US
M01	T29	50	yes	yes	no	No	no	no	no	T29_M01_50_1L_US
M02	T30	30	yes	yes	no	no	no	no	no	T30_M02_30_1L_US

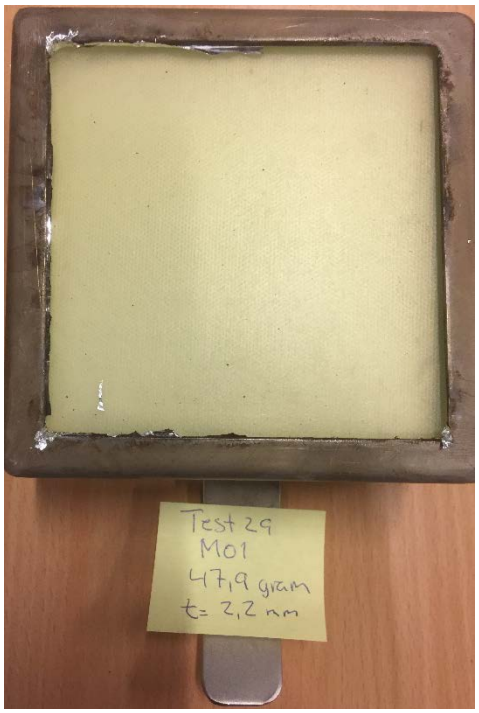

Figure 61. T29, M01 in sample holder.

Figure 62. T30, M02 in sample holder.

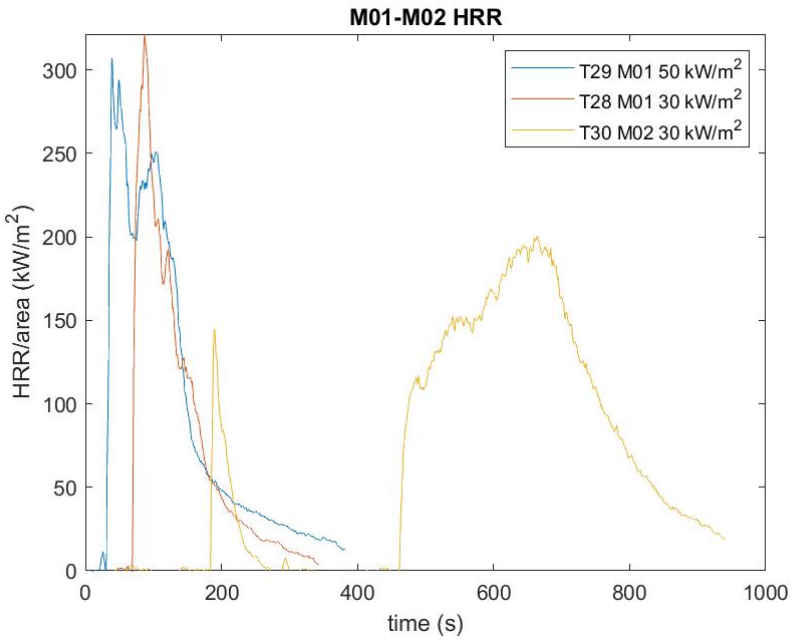

Figure 63. Heat release rates per unit area of insulating plastic materials, M01-MO2, at different heat fluxes.

The plastic sheet, M01, was tested at two different heat flux levels with a varying time to ignition and heat release rates as presented in Figure 63. The magnet coil M02, in T30, was tested at a heat flux of 30 kW/m^2 with a two-peak signature of the heat release rate with a flameout in between. A plausible explanation for this two-peak signature is that the plastic material that covers the coil is ignited but also melted. The melted plastic material has then to be heated up together with the coil to temperatures that releases combustible gas that can be ignited for the second peak. The following graphs, Figure 64 and Figure 65, show the mass loss rates and obscuration for the tests.

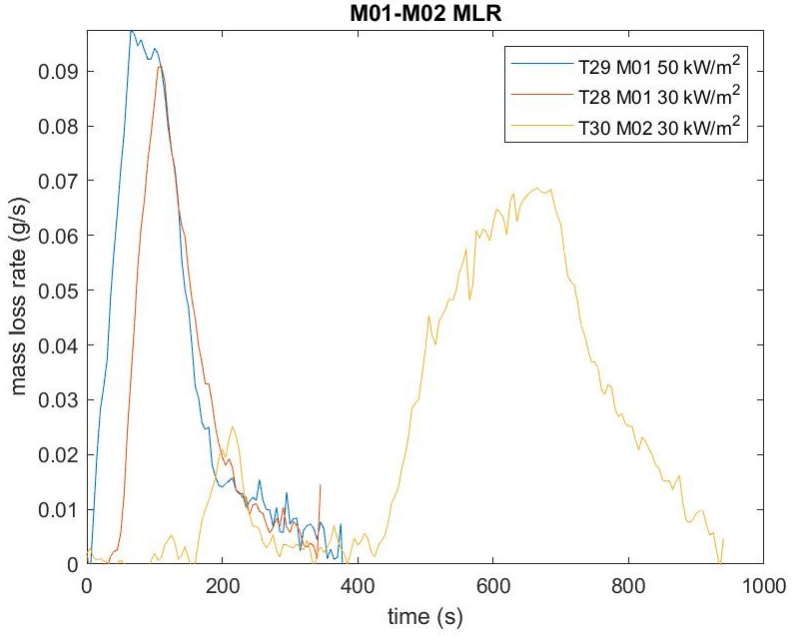

Figure 64. Mass loss rate of isolating plastic materials, M01-M02, at different heat fluxes.

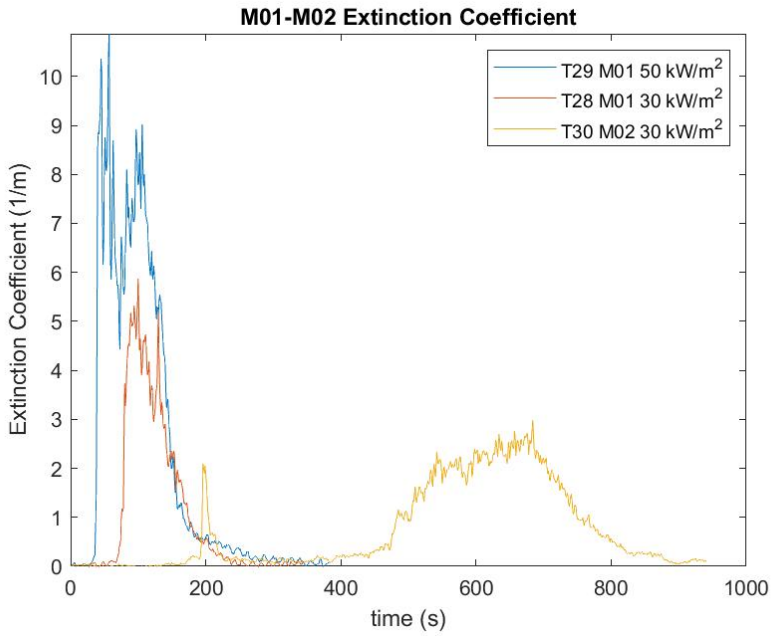

Figure 65. Obscuration of plastic materials, M01-M02, at different heat fluxes.

Figure 66 shows the time dependent values of heat of combustion during each test.

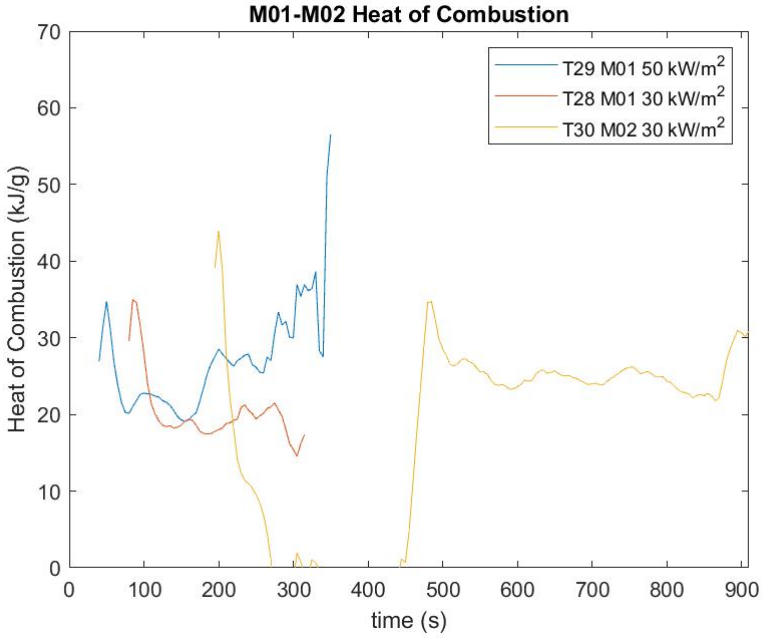

Figure 66. Heat of Combustion from ignition to 30 seconds before end of test.

In Table 28, the resulting fire properties are presented for each test. The yields and heat of combustion are calculated as average values for the test.

Table 28. Fire properties of an insulating plastic material, M01, at different heat fluxes.

Material	Test	Heat flux [kW/m2]	Time to ignition [s]	CO2-yield [kg/kg]	CO-yield [kg/kg]	Heat of Combustion [MJ/kg]
M01	T28	30	77	1.51	0.059	20.14
M01	T29	50	36	1.65	0.063	22.71
M02	T30	30	192/470	1.72	0.039	23.50

2.15 OIL, O01

Oil, O01, is an oil used in Isolde target area. The sales marking is Oil P3: D-35614 Asslar. The oil was tested in three tests as presented in Table 29. Two of these tests, T58 and T61, were performed in the vitiated air chamber, VAC.

Table 29. Performed tests of O01.

Test	Heat flux [kW/m^2]	Depth [mm]	DMS	AETHALO-METER	DGI	APM	TEM	ICP-MS	VAC	File name
T35	30	5	yes	yes	no	no	no	no	no	T35_O01_30_5mm
T36	30	10	yes	yes	no	no	no	no	no	T36_O01_30_10mm
T37	20	5	yes	yes	yes	yes	yes	yes	no	T37_O01_20_5mm

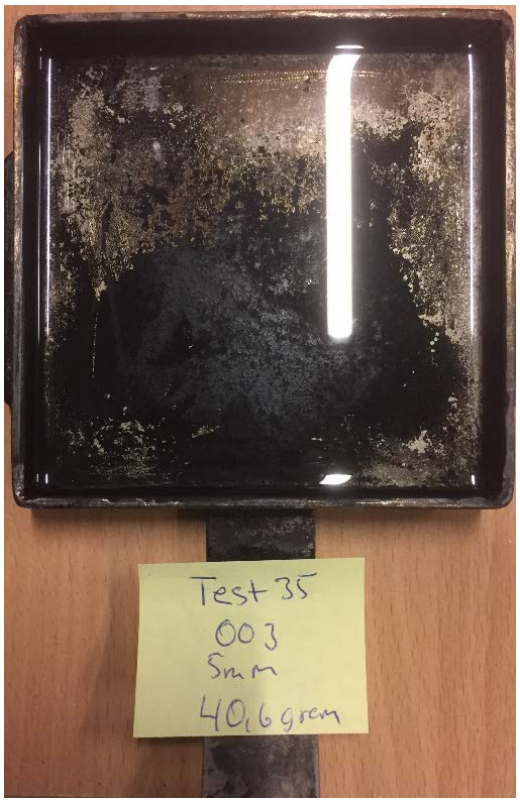

Figure 67. T35, in sample holder.

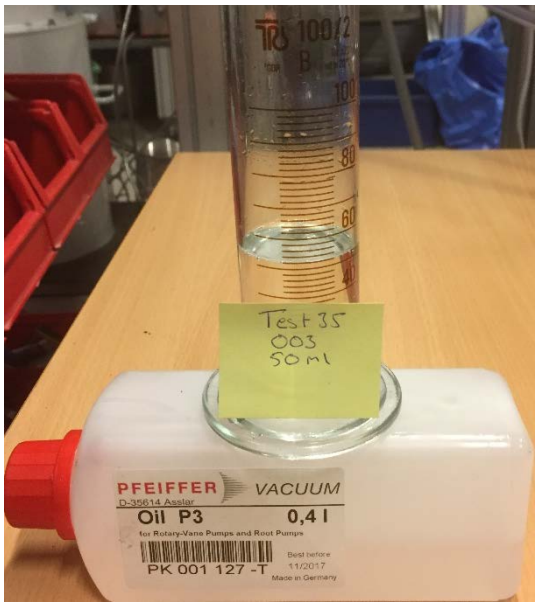

Figure 68. T35, with container.

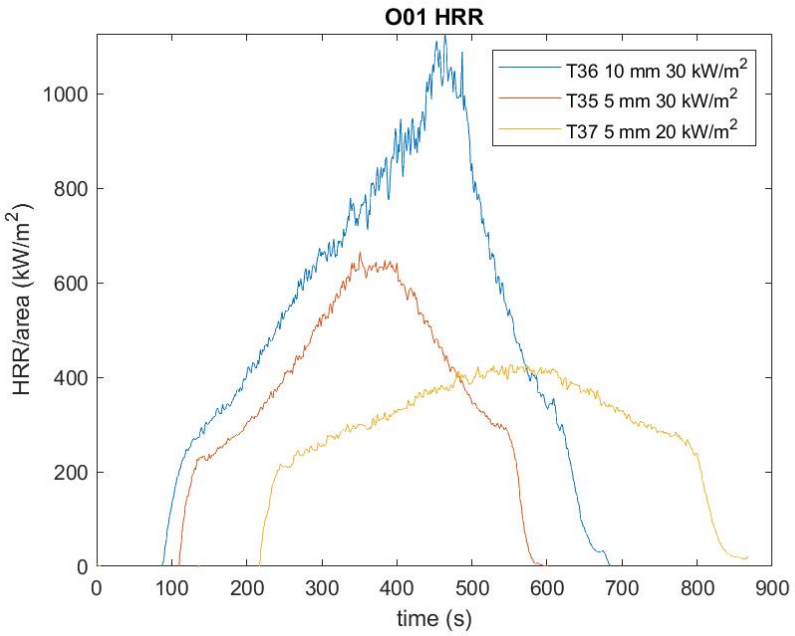

Figure 69. Heat release rates per unit area of an oil, O01, at different heat fluxes and sample depths.

Resulting heat release rates of the oil was among the largest of the products and materials in the test as presented in Figure 69. T35 was initially intended to be performed with 10 mm oil depth at 50 kW/m^2 but was changed to 5 mm depth and 30 kW/m^2 to compare with T36 that was performed with the same heat flux but with 10 mm oil depth. Comparison between T35 (5 mm depth) and T36 (10 mm depth) shows that the peak heat release is twice as high due to the deeper oil depth in T36. A plausible explanation is that the heat loss to the sample holder is lower in T36 due to the higher oil depth. This results in a higher burning rate. SFPE Handbook of Fire Protection Engineering [9] shows examples (p. 2578) in higher heat release rates measured for gasoline at higher fuel depths, ranging from 1 to 18 mm.

The following graphs, Figure 70 and Figure 71, show the mass loss rates and obscuration at the tests.

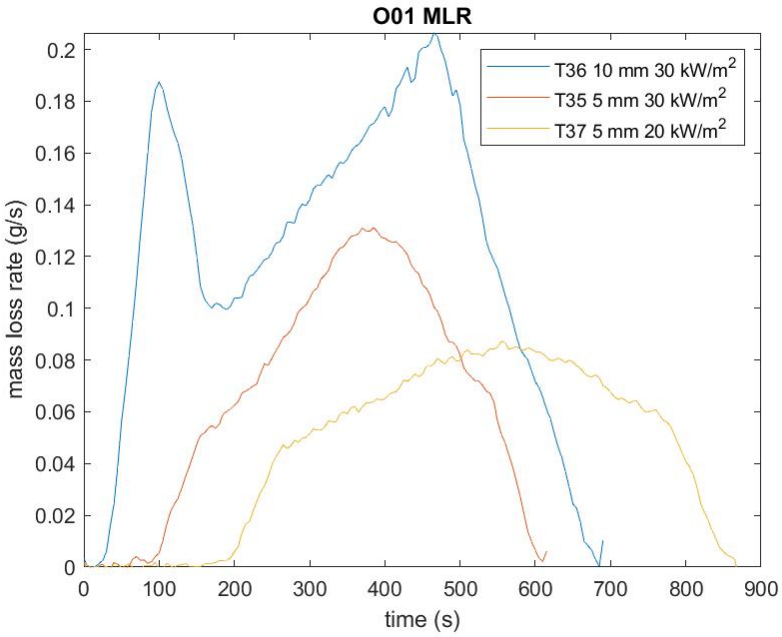

Figure 70. Mass loss rate of an oil, O01, at different heat fluxes.

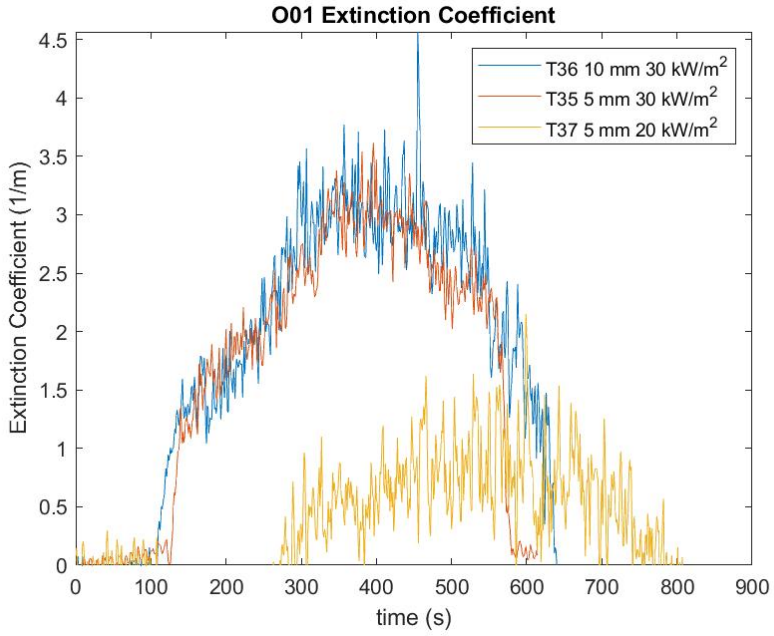

Figure 71. Obscuration of oil, O01, at different heat fluxes.

Figure 72 shows the time dependent values of heat of combustion during each test.

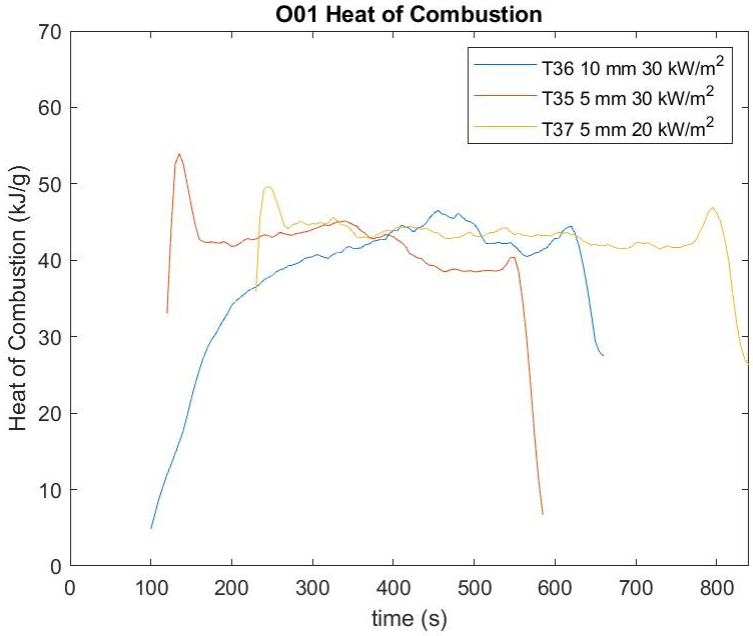

Figure 72. Heat of Combustion from ignition to 30 seconds before end of test.

In Table 30, the resulting fire properties are presented for each test. The yields and heat of combustion are calculated as average values for the test.

Table 30. Fire properties of oil, O01, at different heat fluxes.

Test	Heat flux [kW/m2]	Time to ignition [s]	CO2-yield [kg/kg]	CO-yield [kg/kg]	Heat of Combustion [MJ/kg]
T35	30	119	2.68	0.039	41.11
T36	30	97	2.38	0.033	37.91
T37	20	226	2.59	0.041	43.04

2.16 Plastic materials, P01-P06

Table 31 presents a short description of the plastic materials.

Table 31. Tested plastic materials.

Plastic	Description
P01	Borated polyethylene
P02	Expanded plastic
P03	ABS element
P04	Elements of low density polyethylene foam with a diameter of 16mm
P05	Sheet of PMMA board with a thickness of 3 mm
P06	Sheet of PS board, thickness 4,6 mm

Pictures of the tested plastic materials are presented in the following figures.

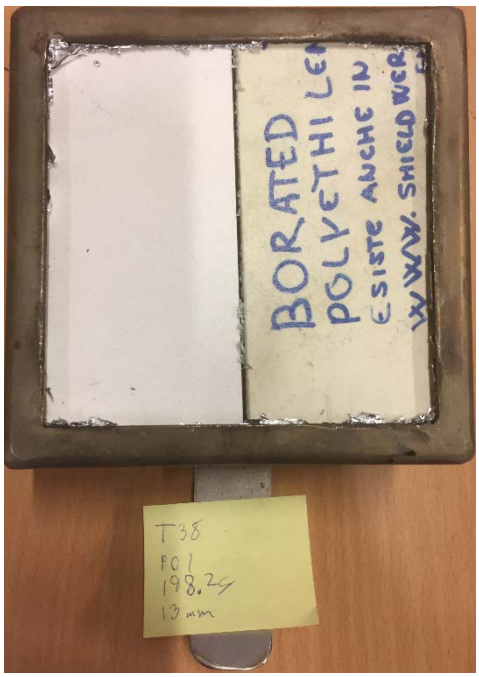

Figure 73. T38, P01 in sample holder.

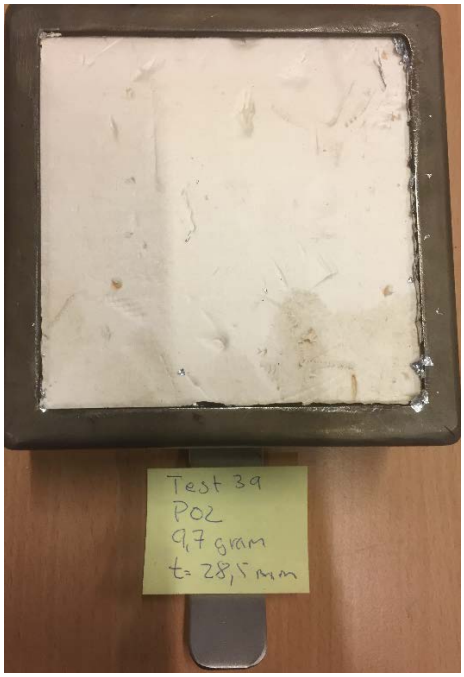

Figure 74. T39, P02 in sample holder.

Figure 75. T40, P03 in sample holder.

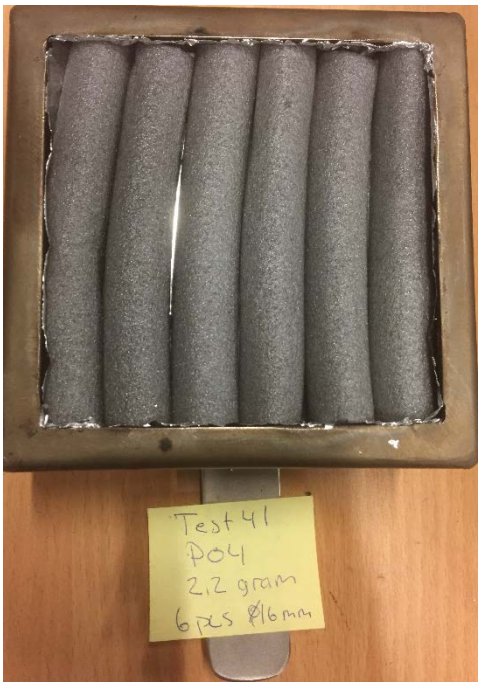

Figure 76. T41, P04 in sample holder.

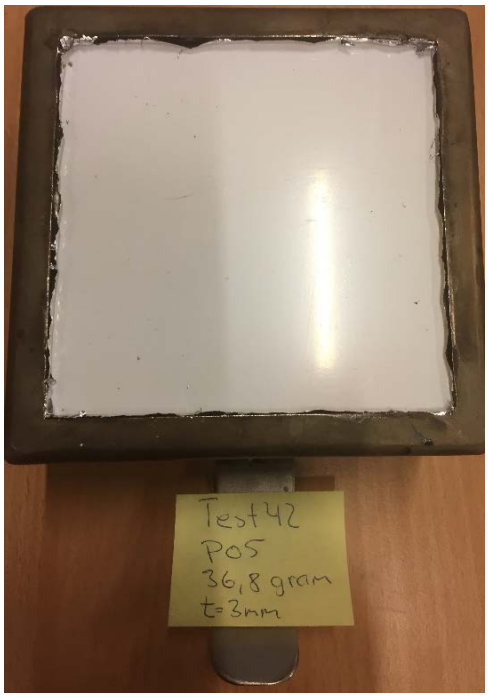

Figure 77. T42, P05 in sample holder.

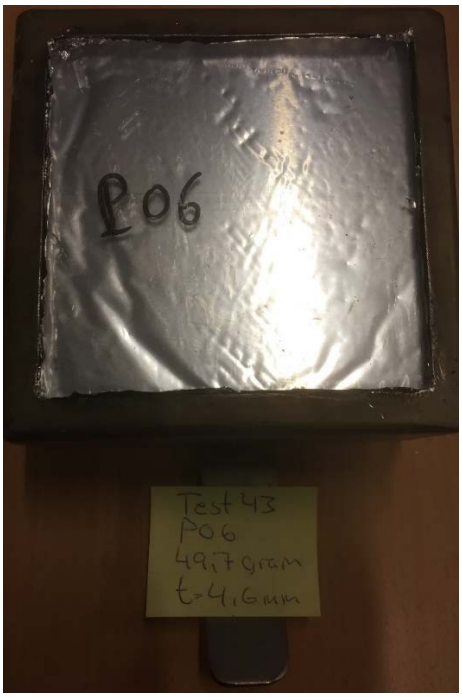

Figure 78. T43, P06 in sample holder.

The plastic materials were tested in single tests and are presented in Table 32.

Table 32. Performed tests of P01-P06.

Plastic	Test	Heat flux [kW/m²]	DMS	Aethalo-meter	DGI	APM	TEM	ICP-MS	VAC	File name
P01	T38	20	yes	yes	yes	no	no	no	no	T38_P01_20_1L_US
P02	T39	20	yes	yes	no	no	no	no	no	T39_P02_20_1L_US
P03	T40	20	yes	yes	no	no	no	no	no	T40_P03_20_1L_US
P04	T41	20	yes	yes	no	no	no	no	no	T41_P04_20_1L_US
P05	T42	20	yes	yes	no	no	no	no	no	T42_P05_20_1L_US
P06	T43	20	yes	yes	no	no	no	no	no	T43_P06_20_1L_US

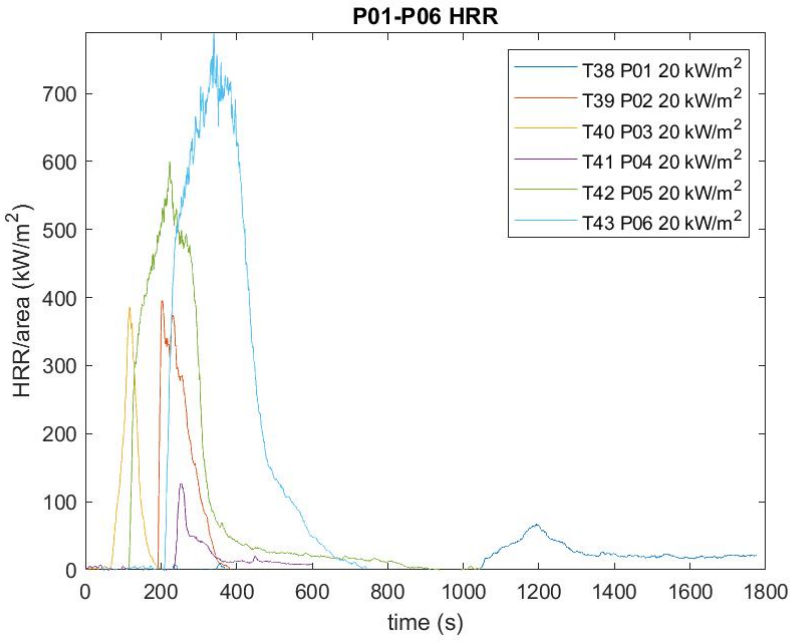

Figure 79. Heat release rates per unit area of plastic materials, P01-P06, at different heat fluxes.

The tested plastic materials results in varying properties of combustibility as presented in Figure 79. The borated polyethylene in P01 has in earlier fire tests [10] shown to have fire retardant properties, which is exemplified here as resulting in the lowest heat release rate. The long time to ignition for P01 relates to a thick sample. Highest combustibility among the tested plastic materials derives to the polystyrene in P06.

The following graphs, Figure 80 and Figure 81, show the mass loss rates and obscuration at the tests.

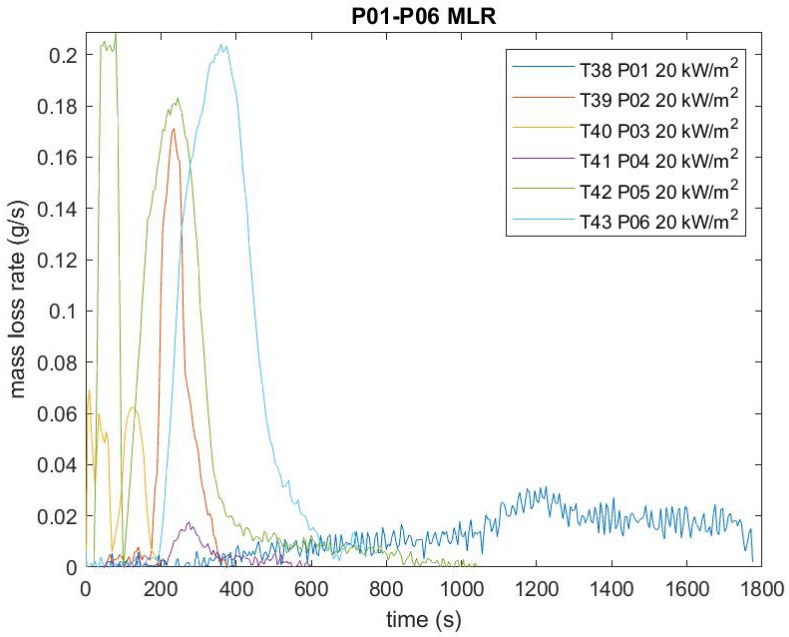

Figure 80. Mass loss rate of plastic materials, P01-P06, at different heat fluxes.

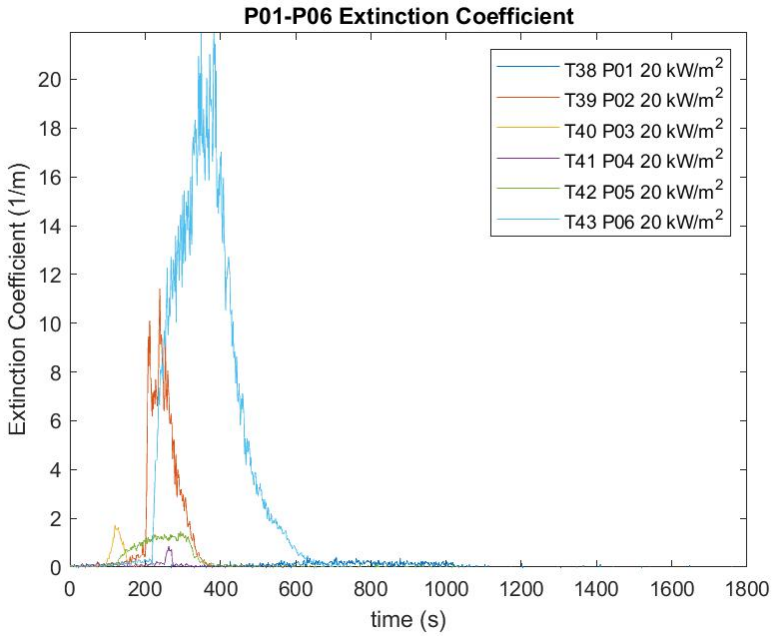

Figure 81. Obscuration of plastic materials, P01-P06, at different heat fluxes.

Figure 82 shows the time dependent values of heat of combustion during each test.

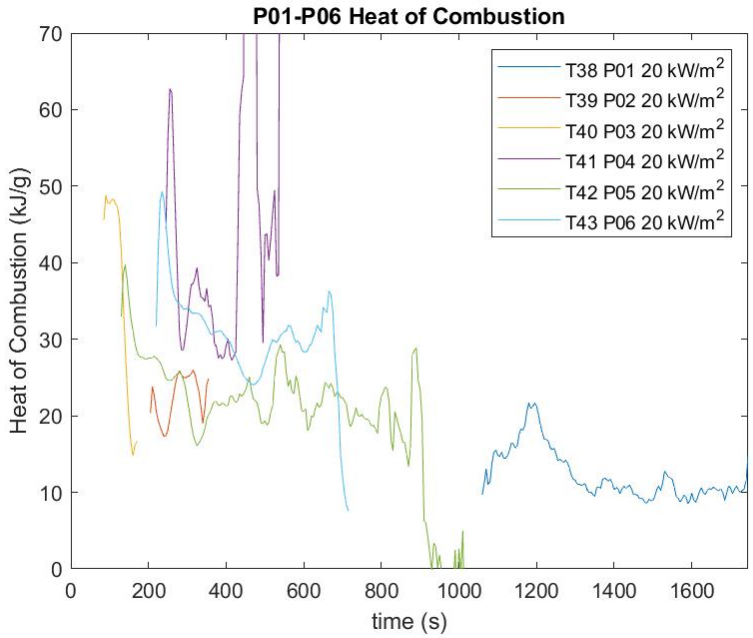

Figure 82. Heat of Combustion from ignition to 30 seconds before end of test.

In Table 33, the resulting fire properties are presented for each test. The yields and heat of combustion are calculated as average values for the test.

Table 33. Fire properties of plastic materials, P01-P06, at heat flux of 20 kW/m^2.

Plastic	Test	Heat flux [kW/m2]	Time to ignition [s]	CO2-yield [kg/kg]	CO-yield [kg/kg]	Heat of Combustion [MJ/kg]
P01	T38	20	1055	1.07	0.056	12.18
P02	T39	20	203	1.28	0.043	18.72
P03	T40	20	81	2.47	0.024	38.06
P04	T41	20	244	1.98	0.049	34.74
P05	T42	20	126	2.10	0.014	24.94
P06	T43	20	216	2.31	0.065	31.05

2.17 Repeatability

The standard of ISO 5660:2015 [5] includes a repeatability formula for the HRR for cone calorimeter tests in the range of 70-1120 kW/m^2. This formula is applied to the three repeated tests, T4-T22-T52 of Cable 4 presented in Figure 17. Using the formula leads to the probability of 95 % that repeated tests will be within ± 30kW/m^2, which is the actual case at comparison. The conducted tests are therefore seen as to show good repeatability.

2.18 Critical heat flux

The results from the calculations of Janssens method is shown in Table 34.

Table 34. Presenting the calculated minimum critical heat fluxes required for ignition.

Cable	Cable diameter [mm]	Critical heat flux [kW/m^2]
C01	9.3	10
C02	14	8.5
C04	5	(0.4) Not applicable
C05	7	(5) Not applicable
C07	19	9.5
C08	9.5	(4.6) Not applicable
C10	7.5	8

Evaluation of the calculated results in Table 34 leads to that the method at least do not work for thinner cables such as C04, C05 and C08. These apparently cannot be assumed to be thermal thick as they result in unreasonably low values for the critical heat flux. Nevertheless, the results for the cables with larger diameters show that estimating the minimum critical heat fluxes of the presented cables can be set just under 10 kW/m^2. All the presented cables in Table 34 were ignited at the lowest heat flux, 20 kW/m^2, performed during the testing campaign. Some cables as cable 3 and cable 9 did not ignite at 20 kW/m^2 during the elapsed test time, which was 1555 seconds and 1947 seconds. Unfortunately, there were only two ignited tests of both these cables which is not appropriate enough to determine the critical heat flux according to the test method and thereby not presented in Table 34.

3 Conclusion

- Tests at well-ventilated conditions were performed at an incident heat flux of 20-30-50 kW/m^2. At these conditions, peak heat release rates were measured at 50 kW/m^2 as follows:
  - Oil, 1100 kW/m^2
  - Cables 350 kW/m^2
  - Plastic materials, 800 kW/m^2
- Significant for most of the cables was a heat release rate curve with two distinct peaks. This could be due to the outer combustible jacket burning first followed by the interior plastic insulating material of the cables burning. There could also be heat transfer effects and cracking the material surface contributing to the two peaks. At low incident heat fluxes though, some cables only had a one-peak signature as the plastic insulation material of the cables not was ignited within the test time.
- Critical heat flux was calculated for some cables to be just below 10 kW/m^2.

4 References

1. NIST. *Cone Calorimeter*. [cited 2017 December 1]; Available from: https://www.nist.gov/laboratories/tools-instruments/cone-calorimeter.
2. Technology, F.T. *Controlled Atmosphere Attachment*. [cited 2019 April 18]; Available from: http://www.fire-testing.com/Controlled-atmosphere-attachment.
3. Werrel, M., et al., *The calculation of the heat release rate by oxygen consumption in a controlled-atmosphere cone calorimeter*. Fire and Materials, 2014. **38**(2): p. 204-226.
4. STANDARDIZATION, E.C.F., *Plastics – Simple heat release test using a conical radiant heater and a thermopile detector (ISO 13927:2015)*. 2015, EUROPEAN COMMITTEE FOR STANDARDIZATION.
5. International Organization for Standardization, *ISO 5660-1:2015 Reaction-to-fire tests - Heat release, smoke production and mass loss rate* 2015.
6. Babrauskas, V. and S. J Grayson, *Heat Release in Fires*. 1992.
7. Janssens, M., *Thermal model for Piloted Ignition of Wood Including Variable Thermophysical Properties*, in *Third International Symposium on Fire Safety Science*. 1991: Edinburgh, Scotland. p. 167-176.
8. Janssens, M., *Analysis of cone calorimeter ignition data: A reappraisal*, in *Interflam 2013*. 2013: Royal Holloway College, UK.
9. Hurley, M.J., *SFPE handbook of fire protection engineering*. 2016: New York : Springer, cop. 2016. 5 edition.
10. Dan Madsen, F.J., Patrick van Hees, *Borated polyethylene - Fire properties and other issus*, in *Division of Fire Safety Engineering*. 2014, Lund University.

5 Appendix

Item	Code	Description	Manufacturer	Source	Colour	Marking and commercial name	Ø[mm]	CERN reference	Why selected
Cables	C01	Multi conductor cable with thermoset insulator	DRAKA	CERN Shop	blue	DRAKA 14W20 CERN MCA 14 IEC 60332-1 ZERO HALOGEN 09 3212577 405130804 3160 MT	9.3	04.21.48.314.1	CERN-CFT-P1
	C02	Multi conductor cable with thermoset insulator	ELETTRONICA CONDUTTORI	CERN Shop	black	ELETTRONICA CONDUTTORI - 13W19 - CERN PG5SJ - IEC 60332-3-24 ZERO HALOGEN MT 0782	14	04.08.61.529.8	CERN-CFT-P1
	C03	coax cable with thermoplastic dialectric insulator	DRAKA	CERN Shop	red	DRAKA 17W11 CCH50 IEC 60332-3-24 17W11 CCH50 IEC 60332-3-24 09 3214535 703151200 1188 MT	10.3	04.31.51.705.6	CERN-CFT-P1
	C04	coax cable with thermoplastic dialectric insulator	DRAKA	CERN Shop	brown	DRAKA 2016 CB 50 09 3414713 6111308426187 MT	5	04.61.11.225.6	CERN-CFT-P1
	C05	Multi conductor cable with thermoset insulator	DRAKA	CERN Shop	white	DRAKA 16W04 CERN NE2 IEC 60332-1 ZERO HALOGEN 09 3213839 601291328 3876 MT	7	04.21.52.100.2	CERN-CFT-P1
	C06	-	-	CERN Shop		CAB.SIG.BL.13x2x0.50mm2 NE26	-	04.21.52.140.4	Most sold one

Item	Code	Description	Manufacturer	Source	Colour	Marking and commercial name	Ø[mm]	CERN reference	Why selected
Cables	C07	white thick	-	CERN Shop		CAB.SIG.BL.24x2x0.50mm2 NE48	19	04.21.52.150.2	Most sold one
	C08	ORANGE small thicker	-	CERN Shop		CABLE ANTIFEU 2x1.5mm² MHF2	9.5	04.08.05.215.7	Most sold one
	C09	Orange, 2cm D	-	CERN Shop		CAB.SIG.BL. 24x2x1.5mm² NHF48	34.5	04.21.53.348.6	Hi-Lumi/Jose
	C10	ORANGE small thinner	-	CERN Shop	-	CAB.SIG.BL. 1x2x0.75mm² NFF2	7.5	04.21.53.155.7	Hi-Lumi/Jose - Most sold one
	C11	BLACK rigid	-	CERN Shop	-	FLEX.COPPER CABLE 150 mm2	23	04.08.61.985.8	Hi-Lumi/Jose
	C12	BLACK	-	CERN Shop	-	CABLE Cu FLEX. 5x16mm ² PN5SJ	22	04.08.61.591.2	Hi-Lumi/Jose
Magnets	M01	Samples of material used to isolate magnets.	-	TE-MSC /J. Bauche	-	STRAT.GLASS FABR.SHEET E 2	-	44.88.75.120.6	In Vincze study, one of the most combustible item in SPS. Potentially activated
	M02		-	TE-MSC /J. Bauche	-	SPS magnet coil	-	-	Combustible item in magnets. Potentially activated

Item	Code	Description	Manufacturer	Source	Colour	Marking and commercial name	Ø[mm]	Why selected
Electrical	E01	PLC electrical board 1	-	Old EPC recup service	-	-	-	Standard PLC material present in power converters, control boards and racks
	E02	PLC electrical board 2	-	Old EPC recup service	-	-	-	Standard PLC material present in power converters, control boards and racks
	E03	PLC electrical board 3	-	Old EPC recup service	-	-	-	Standard PLC material present in power converters, control boards and racks
	E04	PLC electrical board 4	-	Old EPC recup service	-	-	-	Standard PLC material present in power converters, control boards and racks
Plastic	P01	Borated PE	-	Fabio Archive	-	-	-	-
	P02	Expanded XX	-	Fabio Archive	-	-	-	-
	P03	ABS elements different width	-	LM	-	-	-	-
	P04	PE low density foam	Tramicord	LM	grey	Low Density Polyethylene	16mm	Low density PE representative
	P05	PMMA boards white translucid	-	LM	-	PMMA	-	-
	P06	PS boards transparent	-	LM	-	PS	-	-
Oil	O01	Oil Used in Isolde target area (new sample, not contaminated)	PFEIFFER	TE/VSC. Jose Ferreira	-	Oil P3: D-35614 Asslar	-	FIRIA pilot case. General request from Project Board